

# **Intertidal Soundscapes of Hardened and Living Shorelines: A Case Study of Habitat Enhancement**

Audrey Looby<sup>1,2\*</sup>, Laura K. Reynolds<sup>3</sup>, Ashley M. McDonald<sup>2,3</sup>, Savanna Barry<sup>1,2</sup>, Mark Clark<sup>3</sup>,  
Charles W. Martin<sup>2,4</sup>

<sup>1</sup>Fisheries and Aquatic Sciences, Institute of Food and Agricultural Sciences, University of Florida, Gainesville, FL 32611, U.S.A.

<sup>2</sup>Nature Coast Biological Station, Institute of Food and Agricultural Sciences, University of Florida, Cedar Key, FL 32625, U.S.A.

<sup>3</sup>Soil, Water, and Ecosystem Sciences, Institute of Food and Agricultural Sciences, University of Florida, Gainesville, FL 32611, U.S.A.

<sup>4</sup>Dauphin Island Sea Lab, University of South Alabama, Dauphin Island, AL 36528, U.S.A.

\*Corresponding author (Email: [alooby101@gmail.com](mailto:alooby101@gmail.com); Tel. +19086421151;  
<https://orcid.org/0000-0003-1833-8643>)

## ABSTRACT

1. Organisms, such as fishes and invertebrates and including their larval stages, listen to underwater soundscapes to detect information about nearby habitats. Such soundscapes may be influenced by habitat degradation or enhancement, which can lead to acoustically mediated feedback loops affecting the overall ecosystem.
2. Despite the importance of underwater sounds on ecological functioning, there have been limited studies documenting soundscapes of intertidal ecosystems and few, if any, of living shoreline soundscapes. Living shorelines would especially benefit from acoustically mediated effects for objectives like encouraging fish and invertebrate settlement.
3. This case study used a Before-After-Control-Impact design to sample soundscapes and nekton (i.e., fishes and mobile macroinvertebrates) at a living shoreline construction and a nearby hardened shoreline in Cedar Key, FL (USA). Diel soundscape patterns and acoustic attenuation at the two sites were also described a year following the living shoreline construction.
4. In the acoustic sampling, the high frequency bands of both shorelines were dominated by invertebrate sounds that were influenced by season, site, and time of day, while the low frequency band of the living shoreline was often dominated by a loud anthropogenic sound. About a year after the living shoreline installation—despite similar measured acoustic attenuation at both sites—the living shoreline featured louder sound pressure levels compared to the hardened shoreline, which may be particularly beneficial for promoting foundational species and other organism settlement.

5. These results demonstrate that Gulf of Mexico intertidal habitats may have soundscape differences even within close proximity and that living shorelines may enhance acoustic characteristics in ways beneficial to continued shoreline development. This represents an important step in better understanding the relationships between habitat structures, nekton communities, and their associated soundscapes as well as the application of passive acoustic monitoring to improve coastal management and conservation.

*Keywords:* bioacoustics, ecoacoustics, salt marshes, oysters, riprap, fishes, habitat restoration, anthropogenic noise

## **1 INTRODUCTION**

In the face of increasing threats to the coastal zone and the humans that inhabit or rely on it (Valiela et al., 2001; Waycott et al., 2009; Barbier et al., 2011; Beck et al., 2011; Dahl, 2011; Short et al., 2016; Moore et al., 2020), there have been growing efforts to improve management methods through the construction of living shorelines (Smith et al., 2020). ‘Living shoreline’ is a loosely defined term describing a variety of shoreline stabilization methods that use plants and other natural materials, sometimes in combination with harder structures (e.g., rock sills), to provide habitat value and enhance resilience (National Oceanic and Atmospheric Administration, 2015; Bilkovic et al., 2016; O’Donnell, 2017; Smith et al., 2020). Living shorelines may provide similar or better resistance to landward erosion compared to equivalent natural environments and hardened structures (Gittman et al., 2014; Smith et al., 2018). Because of their long-term persistence and the ability of their living elements to repair and adapt to changing conditions,

living shorelines can further promote lateral accretion of shoreline zones (Chowdhury et al., 2019; Polk et al., 2022). In addition to their protective value, living shorelines often have the added benefit of providing enhanced habitat to organisms and can have similar or greater species diversity, food web support, and abundance of fishes and crustaceans (Gittman et al., 2016a; Isdell et al., 2021; Toft et al., 2021; Guthrie et al., 2022). Living shorelines are therefore becoming increasingly recognized as more desirable than hardened shorelines (Gittman et al., 2015; Bilkovic et al., 2016; Gittman et al., 2016b).

While numerous studies have examined the effects of living shorelines on a variety of ecological processes, community metrics, and economic value (e.g., O'Donnell, 2017; Isdell et al., 2021), there have been limited studies about how this habitat enhancement or restoration method may affect the presence of underwater sounds and vice versa. Many organisms, such as fishes and invertebrates and including their larval stages, listen and contribute to underwater soundscapes (i.e., all the sounds in a landscape) to detect and convey information (Pijanowski et al., 2011; Lillis et al., 2014b; Mullet et al., 2017; Salas et al., 2019; Looby et al., 2022; Solé et al., 2023a). Anthropogenic sounds can impact the production and detection of these ecologically relevant sounds as well as the organisms themselves through direct damage, hearing threshold shifts, or masking, among other physiological and behavioral changes (Cox et al., 2018; Duarte et al., 2021; Ledoux et al., 2023; Solé et al., 2023a, 2023b). At least in part because of differences between sound-producer abundances, natural and restored habitats, such as sponge reefs, coral reefs, and hard-bottom habitats, may have increased soundscape volume and complexity compared to degraded habitats—with improved ecological functioning provided by sounds (Butler et al., 2016, 2017; Archer et al., 2018; Lyon et al., 2019; Lamont et al., 2022).

Furthermore, acoustic enrichment of degraded habitats through the playback of sounds of healthy ecosystems has also been found to enhance recruitment and habitat building in several ecosystems, including subtidal oyster reefs and coral reefs (Gordon et al., 2019; Williams et al., 2021, 2022; McAfee et al., 2023). These relationships can create positive feedback loops leading to acoustically mediated ecosystem recovery (Gordon et al., 2019). Living shorelines could especially benefit from such effects through increases to foundational species, such as oysters which settle in response to habitat-associated acoustic cues (Figure 1; Lillis et al., 2014b; Ridge et al., 2015; Chowdhury et al., 2019; McAfee et al., 2023; Williams et al., 2022).

In contrast with some of the more acoustically well-studied ecosystem types that are dominated by harder habitat structures (e.g., oyster shells, coral skeletons) and that occur subtidally, living shorelines are often dominated by plant material and occur in shallow or intertidal zones, which can impact how sound travels and attenuates (Miksis-Olds & Miller, 2006; Biggs & Erisman, 2021; Hauptert et al., 2023; Lee et al., 2023). Air associated with plants from photosynthetic bubble production, internal lacunae, and gas transport systems can dampen sounds traveling through them, with accordingly greater effects with increased density (Arenovski & Howes, 1992; Maricle & Lee, 2002; Miksis-Olds & Miller, 2006; Felisberto et al., 2015; Hopson, 2019; Lee et al., 2023). Other environmental factors, such as temperature, salinity, and water depth, can also have impacts on transmission loss, limiting the distance ecologically relevant signals can travel (Miksis-Olds & Miller, 2006; Biggs & Erisman, 2021; Hauptert et al., 2023). The extent of these environmental effects on acoustic attenuation would influence how much living shoreline soundscapes would increase in detectable volume or complexity given an expected increase in the abundance and diversity of sound-producers. Additionally, the propagation of sound in

shallow water is complicated by the high amounts of environmental variation and interactions between boundary layers, making it more complex to model than deeper water environments (Etter, 1995; Miksis-Olds & Miller, 2006). Sounds produced nearby in air may be more detectable in shallow environments, as well, because of their relative proximity (e.g., Cartolano et al., 2020). Due to these potential factors, it is important to document both soundscapes and attenuation to determine if acoustically mediated effects could benefit living shoreline habitat enhancement or restoration (Figure 1).

The purpose of the case study described herein was to provide a preliminary description of what effects a living shoreline construction may have on its underwater intertidal soundscape (hereafter, simply intertidal soundscape). Using a Before-After-Control-Impact (BACI) approach, intertidal soundscapes and nekton (i.e., fishes and mobile macroinvertebrates) communities were compared between the site of a living shoreline construction and a nearby hardened shoreline reference site. Diel soundscape patterns and acoustic attenuation at the two sites were also assessed a year following the living shoreline construction.

## **2 METHODS**

### **2.1 Site Description**

Sampling took place at the G Street Living Shoreline Restoration, created as part of the Daughtry Bayou Shoreline Project in Cedar Key, FL (USA). The living shoreline construction site was compared to an adjacent hardened shoreline reference site (Figure 2a). The hardened shoreline

was made of riprap (i.e., boulders formed into a wall) installed around 1970 (Olsen Associates, Inc., 2007; Figure 2b). The living shoreline site prior to construction was also a hardened shoreline, made of a slab of flat concrete that sloped up to the sidewalk (Figure 2c). The intertidal substrate immediately adjacent to both shorelines was composed of sand and broken shell with scattered rock and concrete fragments with an approximate density of 15% live oyster cover prior to living shoreline construction (Figures 2b and 2c). Mangroves and seagrasses were absent from the sites. Cedar Key experiences semi-diurnal, mixed tides, with high tide falling at a similar time of day every two weeks. Both the hardened and living shoreline sites are exposed during low tide and submerged by all but the lowest high tides.

The Daughtry Bayou Shoreline Project sought to restore some of the ecosystem services and functions once provided at the living shoreline site, including aiding in the protection of nearby businesses and properties (Figure 2a). Aerial photography from 1951 showed that G Street originally had a sand spit extending into the water, which likely protected the shoreline from erosion until it slowly diminished over time. The initial living shoreline construction occurred throughout the week of 10 August 2020, when two castle block point bars were deployed, an oyster sill was constructed out of 90 reef prisms, sand was used to fill the nearshore area, and then a total of 5,030 plants (primarily *Spartina alterniflora* and *S. patens*, also with *Distichlis spicata*, *Panicum amarum*, *Uniola paniculata*, and *Helianthus debilis*) were planted. In the week of 17 May 2021, additional reef prisms and plants were added to strengthen and stabilize the site (Figure 2d). Though the project sought to return sand and salt marsh plants to an area where they had previously existed, for the purposes of this study, the living shoreline is referred to as a construction project and habitat enhancement rather than restoration because of the use of

artificial, hardened structures in the form of castle blocks and reef prisms. Additional aerial and site photos of the living shoreline construction as well as a timeline of the constructions in relation to the different sampling methods are provided in the Supporting Information (Figures S1–S3).

## 2.2 BACI Sampling

### 2.2.1 Snapshot Acoustic Recordings

Snapshot acoustic sampling followed a Before-After-Control-Impact (BACI) methodology. Sampling took place from 10 November 2019 through 20 August 2021, and occurred at the hardened and living shoreline sites at two locations each (Supporting Information Figure S4). Sampling occurred anywhere from 1.5 hours before to 1 hour after predicted high tide. Actual tide conditions meant sampling ranged from 1.65 hours before to 1.03 hours after measured high tide and between 8:00 am and 1:15 pm (Eastern Time). Predicted tide information was taken from the Windfinder iPhone Application, while measured tide information came from the Cedar Key National Oceanic and Atmospheric Administration (NOAA) tide gauge (#8727520) located 0.5 km from the site. The time of day and tidal cycle were selected to correspond to the nekton monitoring protocol, which also occurred during the day with high tide falling sometime around midday. All four sampling locations were recorded within 1.2 hours from the first to last location. Recorders were deployed at a spot within 1 m of the same location for each sampling. Locations were sampled in a randomized order for each sampling event. Wind speed was measured with a Proster TL017 Handheld Anemometer or a BTMETER BT-100 Handheld



Anemometer over a 30-second duration prior to deployment at each location. Average wind speed never exceeded 5 m/s (~10 knots). Acoustic sampling at the sites was conducted every 2–12 weeks (average 4.2 weeks), dependent on tidal cycle; weather; sufficient water depth; limited nearby foot traffic and recreational usage; and a lack of technical issues with the recording equipment. There were 21 sampling events included in the analysis.

Recordings were obtained using a SQ26-H1 Portable Underwater Recording System (Cetacean Research Technology) made up of a pre-amplified SQ26-08 hydrophone with a sensitivity of -168.19 dB re 1V/ $\mu$ Pa, a frequency range of 0.020–50 kHz, and a flat full-scale frequency response rate between 0.1 and 22 kHz ( $\pm 3$  dB) connected to a solid-state digital recorder (Zoom H1) generating .WAV files. The recording system and settings were kept constant and the input volume on the Zoom recorder was maintained at a fixed level for every recording, so relative received sound pressure levels (SPL) could be compared. Received SPL, measured in decibels (dB), is a logarithmic measure of the ratio of sound pressure relative to a reference value (1  $\mu$ Pa for underwater ecosystems); may be calculated irrespective of a known source location; and is frequently used as an acoustic indicator to describe soundscapes (Lindseth & Lobel, 2018; Monczak et al., 2019; Halliday et al., 2020; Miksis-Olds et al., 2021; Vieira et al., 2021; Wall et al., 2021). As the digital recorder in this system could not be submerged in water, the hydrophone was deployed using a PVC stand (Figure 3a), while an observer stood at least 2 m away onshore (Figure 3b) holding the digital recorder and monitoring the sampling for any potential technical or other issues. Recordings at each location were five minutes in duration—hence the use of the descriptive term snapshot—to ensure all four sampling locations could be recorded within a relatively small tidal window. All locations were within 15 cm of absolute

depth (i.e., irrespective of tidal height). Measured depth at the locations ranged from 15–70 cm due to tidal changes that occurred during and between sampling events, though the depths of the locations never varied more than 30 cm in depth during an individual sampling event.

Temperature and salinity were measured with a YSI ProDSS and its associated calibrated probes after each recording was completed.

### 2.2.2 Nekton Sampling with Fyke Nets and Minnow Traps

Nekton sampling protocols were established as part of the monitoring requirement of the Daughtry Bayou Shoreline Project and also followed a BACI methodology. Nekton sampling efforts were conducted at both the hardened and living shoreline sites using two different gear types, fyke nets and minnow traps, to more effectively capture the species that regularly use intertidal shoreline habitat during the tidal submergence period. Both methods were also selected because their passive collection of nekton caused minimal impact on vegetation compared to more active approaches (e.g., trawls, seines, etc.). Each site had three minnow trap stations, with four baited minnow traps each, placed ~0.5 m apart at each station. Minnow traps were set at mean tide level during high tide to sample small (<15 cm total length) nekton for more effective capture of species with reduced home ranges and high site fidelity (Able et al. 2015). Traps were baited with frozen, locally sourced finfish (wild collections) and left to soak for a minimum of two hours. One fyke net was set at each sampling site ~1.5 meters seaward from the minnow trap stations and used to sample small to medium (<100 cm total length) nekton to ensure capture of transient species that only use the intertidal area when flooded (Figure 3c). Fyke nets were left to soak until outgoing tide dropped water height at the fyke net opening to at least 35 cm to ensure

intertidal habitat drainage and egression of transient nekton species had occurred. All fish and invertebrate nekton species were identified and counted, then released in compliance with ethical regulation protocols (University of Florida Institutional Animal Care & Use Committee Office Protocol #201709978).

Nekton sampling was conducted approximately bimonthly, beginning on 9 September 2019 and ending 1 March 2022, for a total of 14 sampling events (six sampling events before construction and eight after construction). Because the semi-diurnal tidal regime for Cedar Key placed time restrictions on sampling gear deployment, minnow trap and fyke net collections were conducted on separate days, with the two sampling techniques alternated over the course of the two, usually consecutive, days. For example, minnow traps were set at both sites on the first sampling day, then fyke nets were set on the following day. Nekton sampling and acoustic sampling days never co-occurred.

### 2.3 Diel Acoustic Sampling

The diel acoustic sampling (hereafter, diel sampling) aimed to capture soundscapes for a longer time duration than the snapshot acoustic recordings and with high tide falling in four different temporal windows (i.e., approximately at dawn, dusk, midnight, and midday). Sampling occurred in mid-September 2021—13 months following initial living shoreline construction. The dusk recordings were taken around the measured high tide on 12 September 2021 at 7:18 pm, dawn recordings were taken around the measured high tide on 13 September 2021 at 5:24 am, the midnight recordings were taken around the measured high tide on 17 September 2021 at 12:24

am, and the midday recordings were taken around the measured high tide on 17 September 2021 at 11:18 am (Eastern Time). During the week sampling occurred, sunrise was at approximately 7:20 am and sunset was at approximately 7:40 pm (Eastern Time). Sampling was attempted from low to high to low tide, but as the sites were only submerged for part of the time, the sampling captured only a portion of the tidal cycle around high tide.

Recordings were obtained using two  $\mu$ RUDAR-mk2 systems (micro Remote Underwater Digital Acoustic Recorders; Cetacean Research Technology; hereafter  $\mu$ RUDARs). Recorders were made up of a pre-amplified SQ26-08 hydrophone with a frequency range of 0.020–50 kHz and a flat full-scale frequency response rate between 0.1 and 22 kHz ( $\pm 3$  dB) connected to a TASCAM DR-22WL digital recorder generating .WAV files. Each individual  $\mu$ RUDAR was calibrated by the manufacturer shortly before deployment, with each having unique response sensitivities (-170.52 dB re 1V/ $\mu$ Pa used at the hardened shoreline site and -176.55 dB re 1V/ $\mu$ Pa used at the living shoreline site). Recording settings were based on manufacturer recommendations, including a 48 kHz sampling rate, 24-bit file format, 30 gain setting, and mono file type. Recorders were deployed zip tied to concrete blocks at one central location per site (Supporting Information Figure S4), with the hydrophones positioned 3 cm above the substrate. Recorders remained deployed for the two temporal windows occurring within the same 24-hour period to maintain as consistent a position as possible. Both recording locations were within 10 cm of absolute depth. After each recorder retrieval, temperature and salinity were measured with a YSI ProDSS and its associated probes.

## 2.4 Acoustic Attenuation Sampling

Acoustic attenuation (hereafter, attenuation) at the hardened and living shoreline sites was measured in the field using an *in situ*, empirical approach, advocated by and similar to other studies (Miksis-Olds & Miller, 2006; Lillis et al., 2014b; Butler et al., 2017; Hopson, 2019; Wang et al., 2021; Hauptert et al., 2023). Sampling occurred over two days on 1 and 2 November 2021 between 9:50 am and 2:00 pm (Eastern Time). Acoustic recorders and settings were the same as used in the diel sampling. The speaker used to create playbacks was a JBL Clip 3, kept in a watertight plastic bag with sound played over Bluetooth from an iPhone 7, both at full volume. The playback and recording systems and settings were kept constant throughout sampling to be able to compare relative sound level measurements. The sound used for playback was a two-minute broadband (0–24 kHz) Gaussian white noise .WAV file generated in MATLAB (The MathWorks Inc., 2022).

Five transects (3 perpendicular to shore, 2 roughly parallel to shore) were used to characterize attenuation at each site (Supporting Information Figure S4). Transects were sampled in a randomized order. For each attenuation transect, the speaker was placed at the end of the transect closest to shore. One  $\mu$ RUDAR was maintained 1 m from the speaker (i.e., the ‘near’ recorder), while the other  $\mu$ RUDAR was deployed at 1 m, 6 m, 11 m, and 16 m from the speaker (i.e., the ‘far’ recorder) for each attenuation measurement, with the same recorders used for the same positions (near vs. far) for every transect. For each attenuation measurement, two minutes of ambient sound were recorded, then two minutes of speaker playback were recorded. Measurements were not taken if boats or planes were passing near the sites. After each recording was completed, water depth was measured with a ruler at the speaker and both recorders.

Temperature, salinity, and dissolved oxygen were also measured at the speaker with a YSI ProDSS and its associated probes.

## 2.5 Acoustic Analysis

All the data compiled by the different acoustic sampling methods were assessed qualitatively and quantitatively following methods used in similar bioacoustics studies (e.g., Halliday et al., 2020; Vieira et al., 2021). Qualitative visual and aural assessments were conducted in Raven Pro 1.6 (K. Lisa Yang Center for Conservation Bioacoustics at the Cornell Lab of Ornithology, 2023). Such assessments were to ensure there were no technical issues with any of the recordings analyzed. They also were used to produce general descriptions of the soundscapes and discuss possible sound sources recorded at the sites based on prior experience and other available resources (e.g., Looby et al., 2022, 2023a, 2023b). Acoustic recordings were also analyzed using the stand-alone, executable form of the Making Ambient Noise Trends Accessible (MANTA) software to obtain acoustic measurements of SPL (Miksis-Olds et al., 2021). The MANTA software was used to calculate SPL in hybrid millidecade bands within 1-min temporal averaging windows (Miksis-Olds et al., 2021). Calculations incorporated acoustic recording systems and calibration, as reported by their respective manufacturers and following MANTA guidelines for usage (Miksis-Olds et al., 2021).

The acoustic analysis measurement windows varied by sampling method. For the BACI acoustic sampling, for each 5-min recording, three one-minute segments (not necessarily consecutive) were randomly chosen for SPL measurements. If any of the minutes randomly chosen had

technical issues or transient anthropogenic sounds (e.g., boat sounds), then another minute was selected for analysis instead, to be more representative of the ambient soundscape at the sites. For the diel sampling, based on visual and aural assessments of the recordings of when the recorders were fully submerged around high tide, the 90 minutes before and after measured high tide were analyzed for SPL for a total of 181 minutes for each site and temporal window. For the acoustic attenuation sampling, one minute of ambient sound and one minute of speaker playback were analyzed for SPL. The minute analyzed was generally the center minute of the two-minute time windows but was occasionally adjusted to avoid any playback disruptions that may have occurred (Supporting Information Figure S5). The MANTA software produced matrices of measured SPL per hybrid millidecade band and minute that could then be analyzed statistically.

## 2.6 Statistical Analysis

The BACI acoustic sampling data were examined for differences in high and low frequency bands between seasons, sites, before and after the initial living shoreline construction (hereafter, before/after construction), and their interactions, with models determined *a priori* to encompass all the parameters of interest. The recordings were divided into two frequency bands (low: 0.1 kHz–2 kHz; high: 2–22 kHz) based on the flat frequency response band of the acoustic recorder used and preliminary examinations of the recordings for the existence of distinct sound sources in different frequencies. This partitioning allowed separate analyses of largely independent sound sources, similar to methods used in other studies (e.g., Lillis et al., 2014a; Ricci et al., 2016; Archer et al., 2018; Monczak et al., 2019; Bertucci et al., 2020; Halliday et al., 2020; van Geel et al., 2022). One mean SPL measurement was calculated for each sampling deployment and

location by arithmetically averaging the unlogged SPL within the low and high frequency bands and across the three one-minute segments, then converting back to a logarithmic scale (dB; van Geel et al., 2022). Season was defined as warm (i.e., summer; May through October) or cold (i.e., winter; November through April), based on previous definitions of annual seasons for the region (Moore et al., 2020), and was used to encompass multiple related environmental variables, like tidal height and temperature. A generalized linear mixed model with a repeated measure term was created to avoid some of the statistical challenges of BACI designs to meet statistical assumptions (Stewart-Oaten et al., 1992). The mean SPL of both frequency bands fit a gamma distribution (low: shape=73.437925, rate=1.148382; high: shape=60.89164, rate=1.00494; Delignette-Muller & Dutang, 2015) and were tested for nonparametric goodness-of-fit with the Kolmogorov-Smirnov test (Arnold & Emerson, 2011). The models were the same for the low and high frequency bands and included the scaled (without centering) mean SPL as the dependent variable; before/after construction, site, season, and their two-way and three-way interactions as the independent variables; and sampling location as a random effect. The models were tested for whether they significantly described the observed variances by comparing them to null models (only including terms for the dependent variable and the random effect) with analysis of variance (ANOVA) testing.

The BACI nekton sampling data were assessed largely qualitatively due to a high occurrence of zero catches with some outliers. The catches from the minnow traps and fyke nets were used to calculate total abundance, Shannon diversity, Simpson diversity, and species richness, all per soak time hour for each deployment. Minnow trap catches were pooled by sampling location (Budria et al., 2016). To examine community structure among samples with non-zero catch,



community abundance per soak time hour was also visualized with nonmetric multidimensional scaling ordination in two dimensions (Okasanen et al., 2022).

The diel sampling data were examined for differences in the high and low frequency bands between temporal windows and sites, with models also determined *a priori*. The recordings were divided into high and low frequency bands and one mean SPL measurement was calculated for each minute of every sampling deployment using the same methods as the BACI acoustic sampling. A linear mixed model with a repeated measure term was created to statistically test the data's relationships to the variables of interest. For both frequency bands, the models included the mean SPL as the dependent variable, site and temporal window as the independent variables, and sampling deployment as a random effect. The low frequency band model residuals were not normally distributed, so the mean SPL values were log-transformed for the model analysis. The models were tested for whether they significantly described the observed variances by comparing them to null models (only including terms for the dependent variable and the random effect) with the approximate F-test based on the Kenward-Roger approach (Halekoh & Højsgaard, 2014).

The attenuation sampling data were examined for differences between sites and distances away from the speaker. Based on a preliminary assessment of the recordings during speaker playback, the analysis focused on a frequency band of 7–12 kHz and only when the far recorder was at 1 m, 6 m, and 11 m distances from the speaker, to ensure sufficient received playback signals to make meaningful measurements and to avoid frequency cut-off in shallow water (Rogers & Cox, 1988; Miksis-Olds & Miller, 2006; Supporting Information Figure S5). Transmission loss for each deployment (each distance at each location) was calculated as the difference between the

near and far recorders' mean SPL measurements within the selected frequency band, measured in decibels (dB). To statistically test the attenuation sampling data, a linear mixed model with a repeated measure term was created. The model included transmission loss as the dependent variable, site and distance as the independent variables, and transect location as a random effect. The model was tested for significance using the same methods as the diel sampling. A range of expected transmission loss values based on a cylindrical spreading model ( $TL = 10 \log(r) + 10 \log(h)$ , where  $TL$  is transmission loss,  $r$  is the distance between the recorders, and  $h$  is the average water depth of the recorders) was calculated for each distance for comparison (Rogers & Cox, 1988; Miksis-Olds et al., 2006; Erbe & Thomas, 2022). When both recorders were placed 1 m from the speaker, the expected transmission loss between them was assumed to be 0 dB.

All statistical analyses were conducted in R version 4.2.1 (2022-06-23; R Core Team, 2022). All models were created with the package “lme4” version 1.1.30 (Bates et al., 2015). Gamma distributions were established by the function `fitdist` in the package “fitdistrplus” version 1.1.8 (Delignette-Muller & Dutang, 2015). Kolmogorov-Smirnov tests were run with the package “dgof” version 1.4 (Arnold & Emerson, 2011). The ANOVA testing was conducted with the `anova` function. The approximate F-test based on the Kenward-Roger approach was conducted with the `KRmodcomp` function in the package “pbkrtest” version 0.5.1 (Halekoh & Højsgaard, 2014). Post hoc protected non-adjusted pair-wise comparisons were conducted with the package “emmeans” version 1.8.3 (Lenth, 2022). All graphs were created with the package “ggplot2” version 3.4.0 (Wickham, 2023), except for the nonmetric multidimensional scaling ordinations which were created with the package “vegan” version 2.6.2 (Okasanen et al., 2022) and plotted with base R.

### 3 RESULTS

#### 3.1 BACI Sampling

##### 3.1.1 Snapshot Acoustic Recordings

The high frequency band of the BACI acoustic sampling varied primarily by season and the interaction of season and before/after construction—indicating that seasonal trends differed between years—but not by site, before/after the living shoreline construction, or the other interaction terms (Figure 3d; Supporting Information Figures S6 and S7). Similar to other studies of comparable habitats (e.g., Lillis et al., 2014a), the high frequency bands of the recordings from both sites were dominated by high intensity clicking, crackling, or snapping sounds, likely predominantly produced by snapping shrimp from the family Alpheidae (Breder, 1968; Mathews, 2006). The variance in the high frequency band was adequately described by the model ( $X^2(7) = 48.528$ ;  $\Pr(>X^2) < 0.001$ ; Supporting Information Table S1). Season had the greatest effect on the high frequency band mean SPL (F value = 40.723), with the warm season tending to have higher mean SPL compared to the cold season. The interaction of season and before/after construction also had a relatively great effect (F value = 12.457). Other environmental variables, such as temperature and tidal height, tended to fluctuate with season (Figure 3d).

The variance in the low frequency band mean SPL was not adequately explained by model variables ( $X^2(7) = 12.249$ ;  $\text{Pr}(>X^2) = 0.0927$ ; Supporting Information Table S2), but the sites nonetheless showed possibly ecologically relevant differences through the frequent presence of an anthropogenic sound (Figure 4a). The sound was first detected at the fourth sampling event on 18 March 2020, and was detected at all subsequent sampling events except for the one on 10 December 2020. It was not introduced as part of the Daughtry Bayou Shoreline Project. The sound was generally loudest at sampling location 4 (the northernmost location at the living shoreline site), then sampling location 3, and was negligibly if at all detectable at the hardened shoreline sampling locations (Figure 4b; Supporting Information Figure S4). Based on this and additional attempts to pinpoint the location of the source of the sound, it seemed to originate from an abandoned stormwater drainage pipe located just to the north of the living shoreline site (Figure 4c; Supporting Information Figure S4). Other more transient anthropogenic sounds were also occasionally detected, such as those originating from recreational boat traffic as well as possibly low-flying planes departing and arriving from the nearby Cedar Key Airport—though these sounds were not included in the recording segments used in the statistical analysis. Possible fish sounds were found infrequently in the visual and aural examinations of the recordings and their relative contributions to the mean SPL would have been minimal.

### 3.2.2 Nekton Sampling with Fyke Nets and Minnow Traps

The nekton sampling contained many sound-producing species, but data were highly skewed by overall low catch with a few outliers. Of the 25 species caught in the fyke nets and the nine species caught in the minnow traps, at least 14 and six species, respectively, produce detectable

active and/or passive sounds (Berk, 1997; Looby et al., 2022, 2023a, 2023b). Catch and diversity, however, were highly variable and zero-inflated, with eight of the 28 fyke net deployments and 59 of the 84 minnow trap deployments (pooled by sampling location) having zero catch. In terms of species richness, fyke net deployments captured a maximum of nine species and minnow trap deployments captured a maximum of four species. While the catch data may have experienced seasonal variation as well as a possible increase in abundance at the living shoreline site following construction (Figure 3d), the high variance and zero-inflated data prevented the ability to describe and test these potential patterns statistically. Between the sites, seasons, and before/after construction, the community structures were also relatively similar, with some variation between individual samples based on occasional high catch of otherwise rarely captured species, such as *Fundulus grandis*, *Ariopsis felis*, and *Litopenaeus setiferus* (Supporting Information Figures S8 and S9).

### 3.2 Diel Acoustic Sampling

The low and high frequency bands both varied by site, and the high frequency band also varied by temporal window (Figure 5; Supporting Information Figure S10). The variances of both frequency bands were adequately described by their models (low:  $F(4,3) = 16.486$ ,  $p = 0.0221$ ; high:  $F(4,3) = 98.101$ ,  $p = 0.00165$ ). The low frequency mean SPL variance was explained predominantly by site (F value = 59.146) but not by temporal window (F value = 2.266), with the living shoreline site having higher mean SPL. The high frequency mean SPL variance was explained by both site (F value = 118.820) and temporal window (F value = 91.194), with the living shoreline and midday having higher mean SPL. For every deployment, the low frequency

bands remained largely consistent in mean SPL during the 181 minutes recorded and the high frequency bands were generally louder than the low frequency bands, except for the dusk recording deployments, while the high frequency band showed greater variation within the recording deployments (Supporting Information Figure S11). Salinity, temperature, and maximum tidal height were generally similar between sites and among temporal windows (19.85–21.70 ppt, 28.9–30.6 °C, and 1.11–1.47 m respectively).

The frequency bands differed in dominant sound sources. The high frequency band was again dominated by high intensity snapping sounds. Broadband boat sounds were present for some of the recording durations, primarily in the high frequency band and during the midday and dusk time periods. The boat sounds would have contributed to greater mean SPL at the hardened shoreline site because of its closer proximity to the channel the majority of the boats were driving through, while they were less detectable at the living shoreline site. Additionally, and in contrast to the BACI acoustic sampling, the low frequency bands were largely devoid of anthropogenic sounds, including the one likely originating from the abandoned stormwater drainage pipe. Sounds in the low frequency bands were predominantly broadband, short duration click sounds, which occurred at far lower rates than in the high frequency band. Most of these seemed biological in origin, though some may have been the result of objects, like rocks or shells, moving nearby or possibly rubbing against the hydrophone itself. Otherwise, few possible fish sounds were detected.

### 3.3 Acoustic Attenuation Sampling

Attenuation varied by distance but not by site (Figure 6). The model adequately described the variance of the measured transmission loss ( $F(3,17.243) = 7.151, p = 0.00252$ ). Transmission loss did change when the recorders were placed at an increased distance apart as expected ( $F$  value = 11.203) but was similar between the shoreline sites ( $F$  value = 0.102). This shoreline similarity was despite differences observed between individual transects (Supporting Information Figure S5). Mean SPL measured by the near recorder during speaker playback was on average 36 dB higher than the mean SPL of the ambient sound recorded prior to speaker playback. Salinity, temperature, depth at the speaker, and depth at the near recorder were generally similar among deployments (17.56–22.82 ppt, 18.9–23.3 °C, 0.15–0.47 m, and 0.18–0.50 m, respectively), while dissolved oxygen and depth at the far recorder had greater variation (2.28–8.89 mg/L and 0.17–1.05 m, respectively).

#### **4 DISCUSSION**

Based on the results of the case study with additional support from the scientific literature, living shorelines—at least in some circumstances—could be expected to experience acoustically mediated benefits following their construction (Figure 1). In this study, the living shoreline site had an overall higher mean SPL compared to the nearby hardened shoreline reference a year following its construction in both the low and high frequency bands (Figure 5). The sounds that contributed to this mean SPL difference seemed largely biological in origin, likely predominantly snapping shrimp snaps (Breder, 1968; Mathews, 2006). Measured transmission loss, however, was similar between the two sites (Figure 6) and, if anything, attenuation would likely be higher at the living shoreline site because of the presence of salt marsh grasses

(Arenovski & Howes, 1992; Miksis-Olds & Miller, 2006; Felisberto et al., 2015; Hopson, 2019; Biggs & Erisman, 2021; Lee et al., 2023). The detected increase in mean SPL was therefore more likely the result of increased sound-producer abundance and/or sound production rates (Wall et al., 2021; Lillis & Mooney, 2022). Despite our inability to statistically examine nekton community trends, many soniferous species were collected at our living shoreline site and other studies have found increased faunal abundance following living shoreline construction (e.g., Isdell et al., 2021; Guthrie et al., 2022). The measured increase in mean SPL related to biological sounds could lead to further foundational species settlement promoting continued shoreline development and ecological functioning (Lillis et al., 2014b; Ridge et al., 2015; Chowdhury et al., 2019; Williams et al., 2021, 2022; McAfee et al., 2023). The findings also demonstrate that soundscapes associated with distinct intertidal habitats can have meaningful differences, adding to the relatively limited existing literature describing them (McIver et al., 2014).

Several different anthropogenic sounds were present in the soundscape recordings and could contribute to differences between the sites and other environmental parameters. Though it was not present during the diel sampling, the sound tentatively localized as originating from an abandoned stormwater drainage pipe was the most temporally and spectrally prevalent low frequency sound found in the BACI acoustic sampling, particularly at the living shoreline site (Figure 4). Because of its tonal rather than broadband characteristics, it did not contribute enough to detect differences in the mean SPL in the low frequency band in the model, but nonetheless could still represent an ecologically meaningful signal (Cox et al., 2018; Duarte et al., 2021). Sounds from boats and possibly planes passing nearby were also occasionally detected in the various acoustic recordings. Based on observations during the acoustic sampling, some of the



boats and most of the planes passed parallel to both the sites and would have affected them similarly, while other boats, such as most of those observed during the diel sampling, contributed more to the hardened shoreline soundscape because of the site's closer proximity to a boat channel running perpendicular to the south of the sites. In addition to site differences, these anthropogenic sounds could also vary based on times and circumstances of increased human activity—for example, most of the boat sounds in the diel sampling were found in the midday and dusk temporal deployments when boaters were more active. These and other anthropogenic sounds that occur in or near shallow coastal habitats, particularly those adjacent to human communities, may have strong influences on soundscapes and the organisms that rely on them (Hopson, 2019; Cartolano et al., 2020; Duarte et al., 2021; Wilson et al., 2022; Solé et al., 2023a, 2023b).

The high frequency bands of both shorelines were primarily influenced by season in the BACI acoustic sampling. The differences in mean SPL found with season and its interaction with before/after construction could have been related to environmental variables that changed with season and year and could influence sound travel, such as tidal height and temperature (Figure 3d; MacKenzie, 1981). Salinity did not show as strong a seasonal fluctuation (Supporting Information Figure S12) but may also have been an influence on sound travel (MacKenzie, 1981). The variation was likely also related to changes in sound-producer abundance and their sound production behaviors (Monczak et al., 2020). The rates of snapping shrimp snaps and other invertebrate sounds, for example, have been found to be highly correlated with a wide variety of environmental parameters and can vary with even small differences between sites

(Lillis et al., 2017; Lillis & Mooney, 2018; Lillis & Mooney, 2022), in agreement with the findings of this study.

Low frequency bands in similar estuarine habitats tend to be dominated by fish sounds (Lillis et al., 2014a; Ricci et al., 2016), but this was not the case in the acoustic sampling conducted. The acoustic recording methods were likely insufficient to capture all the acoustic variation present at the sites and may have missed fish sounds particularly if they were transient, quiet, or rare (Greenhalgh et al., 2021). The diel sampling would have had a better chance at capturing fish sounds because of the longer recording durations, but the sampling likely occurred outside the spatial or temporal occurrence of fish reproduction sounds that are often easier to detect and can dominate low frequency bands in underwater soundscapes (e.g., Monczak et al., 2019, 2020). The diel sampling encompassed only one week and only occurred over a couple of days. Additional sampling would therefore be required to more comprehensively describe diel, seasonal, and annual soundscape variations, including in both the low and high frequency bands, and determine whether any such variation differs between habitat types.

Despite finding differences between sites in the diel sampling, the BACI acoustic sampling did not find differences between the sites nor before/after construction. The living shoreline construction experienced slow development and some erosion following the initial shoreline construction in August 2020, necessitating additional planting and artificial structure installation in May 2021 (Supporting Information Figure S1). This initially slow establishment may have limited the ability to detect site or before/after differences during the timeline the study was conducted. Environmental metrics associated with living shoreline effectiveness (e.g., fish

diversity and abundance) may take several years before there are detectable changes (Gittman et al., 2016a; Toft et al., 2021) and soundscape changes may therefore be similarly delayed then increase later in the living shoreline's life. The strong seasonal variation found in the high frequency band could have also hindered the ability to detect smaller differences between the other parameters tested.

The nekton sampling found known soniferous species and similar communities between seasons, sites, and before/after construction, but due to zero-inflated data and a restricted timespan for our before/after construction sampling efforts, we were unable to effectively test BACI patterns statistically. Over half of the species caught in the fyke nets and minnow traps are known actively and passively soniferous species (Looby et al., 2022, 2023a, 2023b), including Gulf killifish (*Fundulus grandis*; Drewry, 1962), pinfish (*Lagodon rhomboides*; Caldwell & Caldwell, 1967), black drum (*Pogonias cromis*; Monczak et al., 2019), and white shrimp (*Litopenaeus setiferus*; Berk, 1997). Others may be found to make detectable sound upon further study and many other known soniferous species occur in the region, including snapping shrimp and dozens of other soniferous fishes (Mathews, 2006; Looby et al., 2022). The nekton sampling methods chosen were common to other similar efforts (e.g., Able et al. 2015; Guthrie et al., 2022), but because the nekton sampling catch was zero-inflated with some outliers, the data for the sites examined were too skewed to overcome statistical test assumptions. Also, the monitoring period was established as part of the requirements of the living shoreline project and may have been too limited to detect changes, as restoration effects on macroinvertebrate and fish communities often require from two years to a decade of data collection for detectability when using traditional nekton sampling techniques (Borja et al., 2010). Similar to the challenges found in this study,

living shoreline projects often do not include sufficient long-term monitoring due to funding and logistical constraints, affecting the ability to fully assess living shoreline success and effectiveness (Bilkovic et al., 2016). Daytime sampling with fyke nets and minnow traps may also have limited catch due to gear visibility and avoidance (Smith et al., 2021). These challenges highlight the potential benefits of supplementing traditional sampling methods with acoustic sampling to capture the presence and activities of a greater variety of species as well as overcome the potential limitations of any individual approach.

The methods used to describe attenuation differences between the hardened and living shoreline sites found effects of distance from the speaker but not differences between sites (Figure 6). The cylindrical spreading model tended to overestimate transmission loss compared to what was measured, which could have been the result of the vegetation, the substrate, or a variety of other factors potentially influencing transmission loss at the sites (Rogers & Cox, 1988; Miksis-Olds & Miller, 2006; Erbe & Thomas, 2022). The measurements may also have been influenced by heterogeneous, high-amplitude, ambient sounds or micro-scale differences in recorder position, leading to the variation in received levels detected even when the recorders were placed next to each other at the same distance from the speaker (Figure 6). There was nonetheless still a detectable effect of distance and enough variation between transects to suggest that if the sites had differed greatly in attenuation, such a difference would have been revealed in statistical testing. While some low frequency cut-off in the recordings occurred due to the shallow water depths (Supporting Information Figure S5), this was within the expected frequency range for the substrate at the sites (Rogers & Cox, 1988) and occurred outside of the frequency band used in the acoustic analysis.

Part of the lack of significance on the site-level may have been due to a large portion of the living shoreline site being designated as a recreational beach without any submerged plant structure presence (Supporting Information Figures S1, S2, and S4). Within the salt marsh planting, however, transmission loss would likely be high (Supporting Information Figure S5). Aquatic plant species, such as *S. alterniflora* that was planted at the living shoreline site, can develop complex gas transport and lacunal allocation systems as well as produce bubbles through photosynthesis, with potentially substantial impacts on sound travel (Arenovski & Howes, 1992; Maricle & Lee, 2002; Miksis-Olds & Miller, 2006; Felisberto et al., 2015; Hopson, 2019; Lee et al., 2023). In fact, a similar study in freshwater wetland habitats found significant impacts of both distance and vegetation presence on attenuation (Hopson, 2019). Attenuation through plants may also exhibit seasonal variation related to changes in above-ground biomass and bubble production (Lee et al., 2023). In addition to plants, the introduction of both artificial structures and sand at the living shoreline could have also had meaningful effects on attenuation through changes to sound speed through solid structures, the possible introduction of gas pockets, the scattering properties of different sediments, and variation in effects based on frequency (Nyborg & Rudnick, 1948; Rogers & Cox, 1988; Yang & Tang, 2017; Li et al., 2019; Wang et al., 2021). While not true for this study, it may still be possible that the specific types of habitat structures used in a living shoreline construction could so negatively impact sound propagation that even if more sound producers were present at the site, the overall nearby received sound levels could be similar or lower than if no living shoreline was present (Figure 1). Additional studies are required to validate or refute this possibility.

The research described herein is meant to constitute a case study whose findings should be interpreted with caution and verified in future studies (Bertucci et al., 2020; Greenhalgh et al., 2021). Because the sampling did not have replication in site types (i.e., sampling did not occur at multiple living shoreline constructions and associated reference sites), the results and associated conclusions should not be assumed to be applicable to all living shoreline constructions, even if they are similar in execution (Stewart-Oaten et al., 1992; Underwood, 1992). It is possible that the proximity of the hardened and living shoreline sites, the potential for spillover, the initial limited establishment of the salt marsh grasses, the specific location of the sampling deployments, or other factors may have influenced the results reported. Additionally, soundscape sampling and interpretation, particularly in novel ecosystems, frequently present difficulties in sound source identification, balancing the import of biological and anthropogenic sounds, selecting appropriate sampling methods, and analyzing different acoustic metrics, which may be overcome with additional work (Archer et al., 2018; Bertucci et al., 2020; Greenhalgh et al., 2021; Vieira et al., 2021; van Geel et al., 2022). Challenges associated with the nekton sampling could also be overcome in future studies with longer monitoring time or additional gear types.

There are also limitations in the conclusions that can be drawn on the ecological impacts of the soundscape differences described. Because of logistical constraints with sampling timing and equipment availability, this study focused exclusively on measuring received acoustic pressure levels, not particle motion. Furthermore, in shallow water systems, particle acceleration cannot be accurately estimated from pressure that was measured by a single hydrophone (Solé et al., 2023a). All fishes and many invertebrates can detect the particle motion component of sound and may even rely on it more than acoustic pressure, depending on the species (Nedelec et al., 2016;

Hawkins & Popper, 2017; Popper & Hawkins, 2018; Dinh & Radford, 2021; Salas et al., 2019; Song et al., 2021; Popper et al., 2022; Williams et al., 2022; Solé et al., 2023a). Particle motion may be especially valuable in navigating underwater habitats because it inherently contains directional information in addition to the magnitude, temporal, and frequency information common to both acoustic pressure and particle motion (Song et al., 2021; Solé et al., 2023a). Future work should therefore also document particle motion differences in intertidal zones and the studied shoreline types to provide a more complete picture of the sensory information available to underwater organisms (Nedelec et al., 2016; Hawkins & Popper, 2017; Solé et al., 2023a).

#### 4.1 Implications for Conservation

The results of this case study, notwithstanding its outlined caveats, constitute an important step toward better understanding the interplay between habitat structures, nekton communities, and their associated intertidal soundscapes as well as how these relationships can be applied to monitoring, habitat enhancement, restoration, and conservation objectives. The acoustic sampling found that intertidal soundscapes may have potentially ecologically relevant differences even in close proximity, created by both biological and anthropogenic sound sources. This study with additional support from the literature also suggests that there may be acoustically mediated benefits following a living shoreline construction (Figure 1) that can be utilized to promote management objectives in future living shoreline constructions.

#### **ACKNOWLEDGMENTS**

Funding for this research was provided by the U.S. Environmental Protection Agency under grant number 00D86319; the Florida Fish and Wildlife Conservation Commission and the U.S. Fish and Wildlife Service under award number FL-T-F19AF00403; the University of Florida School of Forest, Fisheries, and Geomatics Sciences; a PADI Foundation Research Grant; and the Doris and Earl Lowe and Verna Lowe Scholarship. The authors are grateful to the Daughtry Bayou Living Shorelines team and volunteers for their construction and monitoring of the shoreline sites, as well as Scott Alford, Adam Searles, Jamila Roth, and Katie Everett for their acoustic sampling field assistance. The authors also thank Micheal Allen, Donald Behringer, and Francis Juanes for their support in planning and executing this research as well as Geraldine Klarenberg for her constructive feedback on the manuscript.

## **ETHICAL APPROVAL**

All procedures performed in the study involving animals were conducted under animal use and care procedure number 201709978 and were in accordance with the ethical standards of the University of Florida Institutional Animal Care & Use Committee Office Protocol.

## **CONFLICTS OF INTEREST**

All authors declare that they have no conflict of interest.

## **DATA AVAILABILITY STATEMENT**



Data are available from the corresponding author upon request.

## References

- Able, K.W., López-Duarte, P.C., Fodrie, F.J., Jensen, O.P., Martin, C.W., Roberts, B.J. et al. (2015). Fish assemblages in Louisiana salt marshes: Effects of the Macondo oil spill. *Estuaries and Coasts*, **38**, 1385–1398. <https://doi.org/10.1007/s12237-014-9890-6>
- Archer, S.K., Halliday, W.D., Riera, A., Mouy, X., Pine, M.K., Chu, J.W.F. et al. (2018). First description of a glass sponge reef soundscape reveals fish calls and elevated sound pressure levels. *Marine Ecology Progress Series*, **595**, 245–252. <https://doi.org/10.3354/meps12572>
- Arenovski, A.L. & Howes, B.L. (1992) Lacunal allocation and gas transport capacity in the salt marsh grass *Spartina alterniflora*. *Oecologia* **90**, 316–322. <https://doi.org/10.1007/BF00317687>
- Arnold, T.A. & Emerson, J.W. (2011). Nonparametric goodness-of-fit tests for discrete null distributions. *The R Journal* **3**(2), 34–39. <https://doi.org/10.32614/RJ-2011-016>
- Barbier, E.B., Hacker, S.D., Kennedy, C., Koch, E.W., Stier, A.C. & Silliman, B.R. (2011). The value of estuarine and coastal ecosystem services. *Ecological Monographs*, **81**(2), 169–193. <https://doi.org/10.1890/10-1510.1>
- Bates, D., Mächler, M., Bolker, B. & Walker S. (2015). Fitting linear mixed-effects models using lme4. *Journal of Statistical Software*, **67**(1), 1–48. <https://doi.org/10.18637/jss.v067.i01>

- Beck, M.W., Brumbaugh, R.D., Airoidi, L., Carranza, A., Coen, L.D., Crawford, C. et al. (2011). Oyster reefs at risk and recommendations for conservation, restoration, and management. *BioScience*, **61**(2), 107–116. <https://doi.org/10.1525/bio.2011.61.2.5>
- Berk, I.M. (1997). Sound production by white shrimp (*Penaeus setiferus*), analysis of another crustacean-like sound from the Gulf of Mexico, and the possible use of passive sonar for detection and stock assessment of shrimp. Master's Thesis, Texas A&M University. Available at: <https://hdl.handle.net/1969.1/ETD-TAMU-1997-THESIS-B46> [Accessed 25 April 2023]
- Bertucci, F., Guerra, A.S., Sturny, V., Blin, E., Sang, G.T. & Lecchini, D. (2020). A preliminary acoustic evaluation of three sites in the lagoon of Bora Bora, French Polynesia. *Environmental Biology of Fishes*, **103**, 891–902. <https://doi.org/10.1007/s10641-020-01000-8>
- Biggs, C.R. & Erisman, B.E. (2021). Transmission loss of fish spawning vocalizations and the detection range of passive acoustic sampling in very shallow estuarine environments. *Estuaries and Coasts*, **44**, 2026–2038. <https://doi.org/10.1007/s12237-021-00914-5>
- Bilkovic, D.M., Mitchell, M., Mason, P. & Duhring, K. (2016). The role of living shorelines as estuarine habitat conservation strategies. *Coastal Management*, **44**(3), 161–174. <https://doi.org/10.1080/08920753.2016.1160201>
- Borja, Á., Dauer, D.M., Elliott, M. & Simenstad, C.A. (2010). Medium- and long-term recovery of estuarine and coastal ecosystems: Patterns, rates, and restoration effectiveness. *Estuaries and Coasts*, **33**, 1249–1260. <https://doi.org/10.1007/s12237-010-9347-5>

- Breder, C.M. (1968). Seasonal and diurnal occurrences of fish sounds in a small Florida bay. *Bulletin of the American Museum of Natural History*, **138**, 329–378.
- Budria, A., DeFaveri, J. & Merilä, J. (2016). Comparison of catch per unit effort among four minnow trap models in the three-spined stickleback (*Gasterosteus aculeatus*) fishery. *Scientific Reports*, **5**, 18548. <https://doi.org/10.1038/srep18548>
- Butler, J., Stanley, J.A. & Butler, M.J. (2016). Underwater soundscapes in near-shore tropical habitats and the effects of environmental degradation and habitat restoration. *Journal of Experimental Marine Biology and Ecology*, **479**, 89–96.  
<https://doi.org/10.1016/j.jembe.2016.03.006>
- Butler, J., Butler, M.J. & Gaff, H. (2017). Snap, crackle, and pop: Acoustic-based model estimation of snapping shrimp populations in healthy and degraded hard-bottom habitats. *Ecological Indicators*, **77**, 377–385.  
<https://doi.org/10.1016/j.ecolind.2017.02.041>
- Caldwell, D.K. & Caldwell, M.C. (1967). Underwater sounds associated with aggressive behavior in defense of territory by the pinfish, *Lagodon rhomboides*. *Bulletin of the Southern California Academy of Sciences*, **66**(1): 69–75.
- Cartolano, M.C., Berenshtein, I., Heuer, R.M., Pasparakis, C., Rider, M., Hammerschlag, N. et al. (2020). Impacts of a local music festival on fish stress hormone levels and the adjacent underwater soundscape. *Environmental Pollution*, **265**(Pt A), 114925.  
<https://doi.org/10.1016/j.envpol.2020.114925>
- Chowdhury, M.S.N., Walles, B., Sharifuzzaman, S., Hossain, M.S., Ysebaert, T. & Smaal, A.C. (2019). Oyster breakwater reefs promote adjacent mudflat stability and salt marsh growth

- in a monsoon dominated subtropical coast. *Scientific Reports*, **9**(1), 8549.  
<https://doi.org/10.1038/s41598-019-44925-6>
- Cox, K., Brennan, L.P., Gerwing, T.G., Dudas, S.E. & Juanes, F. (2018). Sound the alarm: A meta-analysis on the effect of aquatic noise on fish behavior and physiology. *Global Change Biology*, **24**(7), 3105–3116. <https://doi.org/10.1111/gcb.14106>
- Dahl, T.E. (2011) *Status and Trends of Wetlands in the Conterminous United States 2004 to 2009*. U.S. Fish and Wildlife Service. Report to Congress. Available at:  
<https://www.fws.gov/wetlands/documents/status-and-trends-of-wetlands-in-the-conterminous-united-states-2004-to-2009.pdf> [Accessed 25 April 2023]
- Delignette-Muller, M.L. & Dutang, C. (2015). fitdistrplus: An R package for fitting distributions. *Journal of Statistical Software*, **64**(4), 1–34.  
<https://doi.org/10.18637/jss.v064.i04>
- Dinh, J.P. & Radford, C. (2021). Acoustic particle motion detection in the snapping shrimp (*Alpheus richardsoni*). *Journal of Comparative Physiology A*, **207**, 641–655.  
<https://doi.org/10.1007/s00359-021-01503-4>
- Donovan, C. (2014). Oyster larvae. *IAN/UMCES Symbol and Image Libraries*. Available at:  
<https://ian.umces.edu/media-library/oyster-larvae/> [Accessed 25 April 2023]
- Drewry, G.E. (1962). Some observations of courtship behavior and sound production in five species of *Fundulus*. Master's Thesis, University of Texas. Available at:  
<http://hdl.handle.net/2152/23526> [Accessed 25 April 2023]
- Duarte, C.M., Chapuis, L., Collin, S.P., Costa, D.P., Devassy, R.P., Eguiluz, V.M. et al. (2021). The soundscape of the Anthropocene ocean. *Science*, **371**(6529), eaba4658.  
<https://doi.org/10.1126/science.aba4658>

- Erbe, C. & Thomas, J.A. (2022). *Exploring Animal Behavior Through Sound: Volume 1*.  
Springer, Cham
- Etter, P.C. (1995). *Underwater Acoustic Modeling: Principles, Techniques and Applications*.  
CRC Press, Boca Raton
- Felisberto, P., Jesus, S.M., Zabel, F., Santos, R., Silva, J., Gobert, S. et al. (2015). Acoustic monitoring of O<sub>2</sub> production of a seagrass meadow. *Journal of Experimental Marine Biology and Ecology*, **464**, 75–87. <https://doi.org/10.1016/j.jembe.2014.12.013>
- Gittman, R.K., Popowich, A.M., Bruno, J.F. & Peterson, C.H. (2014). Marshes with and without sills protect estuarine shorelines from erosion better than bulkheads during a Category 1 hurricane. *Ocean & Coastal Management*, **102**(Part A), 94–102.  
<https://doi.org/10.1016/j.ocecoaman.2014.09.016>
- Gittman, R.K., Fodrie, F.J., Popowich, A.M., Keller, D.A., Bruno, J.F., Currin, C.A. et al. (2015). Engineering away our natural defenses: An analysis of shoreline hardening in the US. *Frontiers in Ecology and the Environment*, **13**(6), 301–307.  
<https://doi.org/10.1890/150065>
- Gittman, R.K., Peterson, C.H., Currin, C.A., Fodrie, F.J., Piehler, M.F. & Bruno, J.F. (2016a), Living shorelines can enhance the nursery role of threatened estuarine habitats. *Ecological Applications*, **26**(1), 249–263. <https://doi.org/10.1890/14-0716>
- Gittman, R.K., Scyphers, S.B., Smith, C.S., Neylan, I.P. & Grabowski, J.H. (2016b). Ecological consequences of shoreline hardening: A meta-analysis. *BioScience*, **66**(9), 763–773.  
<https://doi.org/10.1093/biosci/biw091>

- Google Earth Pro. (2023). Cedar Key, FL. 29° 08' 06.2"N, 83° 02' 10.8"W, Eye Alt 271 m, Imagery Date February 7, 2020. *TerraMetrics 2023, Google Earth Pro V 7.3.6* [Accessed March 28, 2023]
- Gordon, T.A.C., Radford, A.N., Davidson, I.K., Barnes, K., McCloskey, K., Nedelec, S.L. et al. (2019). Acoustic enrichment can enhance fish community development on degraded coral reef habitat. *Nature Communications*, **10**, 5414. <https://doi.org/10.1038/s41467-019-13186-2>
- Greenhalgh, J.A., Stone, H.J.R., Fisher, T. & Sayer, C.D. (2021). Ecoacoustics as a novel tool for assessing pond restoration success: Results of a pilot study. *Aquatic Conservation: Marine and Freshwater Ecosystems*, **31**(8), 2017–2028. <https://doi.org/10.1002/aqc.3605>
- Guthrie, A.G., Bilkovic, D.M., Mitchell, M., Chambers, R., Thompson, J.S. & Isdell, R.E. (2022). Ecological equivalency of living shorelines and natural marshes for fish and crustacean communities. *Ecological Engineering*, **176**, 106511. <https://doi.org/10.1016/j.ecoleng.2021.106511>
- Halekoh, U. & Højsgaard, S. (2014). A Kenward-Roger approximation and parametric bootstrap methods for tests in linear mixed models – The R package pbkrtest. *Journal of Statistical Software*, **59**(9), 1–32. <https://doi.org/10.18637/jss.v059.i09>
- Halliday, W.D., Pine, M.K., Mouy, X., Kortsalo, P., Hilliard, R.C. & Insley, S.J. (2020). The coastal Arctic marine soundscape near Ulukhaktok, Northwest Territories, Canada. *Polar Biology*, **43**(6), 623–636. <https://doi.org/10.1007/s00300-020-02665-8>
- Hauptert, S., Sèbe, F. & Sueur, J. (2023). Physics-based model to predict the acoustic detection distance of terrestrial autonomous recording units over the diel cycle and across seasons:

- Insights from an Alpine and a Neotropical forest. *Methods in Ecology and Evolution*, **14**(2), 614–630. <https://doi.org/10.1111/2041-210x.14020>
- Hawkins, A.D. & Popper, A.N. (2017). A sound approach to assessing the impact of underwater noise on marine fishes and invertebrates. *ICES Journal of Marine Science*, **74**(3), 635–651. <https://doi.org/10.1093/icesjms/fsw205>
- Hopson, A.M. (2019). Impacts of anthropogenic noise on aquatic invertebrates in wetland habitats. PhD Dissertation, Kent State University. Available at: [https://etd.ohiolink.edu/apexprod/rws\\_etd/send\\_file/send?accession=kent15645874111271&disposition=inline](https://etd.ohiolink.edu/apexprod/rws_etd/send_file/send?accession=kent15645874111271&disposition=inline) [Accessed 25 April 2023]
- Integration and Application Network. (2023). *IAN/UMCES Symbol and Image Libraries*. Available at: <https://ian.umces.edu/media-library/> [Accessed 25 April 2023]
- Isdell, R.E., Bilkovic, D.M., Guthrie, A.G., Mitchell, M.M., Chambers, R.M., Leu, M. et al. (2021). Living shorelines achieve functional equivalence to natural fringe marshes across multiple ecological metrics. *PeerJ*, **9**, e11815. <https://doi.org/10.7717/peerj.11815>
- K. Lisa Yang Center for Conservation Bioacoustics at the Cornell Lab of Ornithology. (2023). Raven Pro: Interactive sound analysis software. Available at: <https://ravensoundsoftware.com/> [Accessed 25 April 2023]
- Kraeer, K. & Essen-Fishman, L.V. (2008). *Lutjanus griseus* (gray snapper). *IAN/UMCES Symbol and Image Libraries*. Available at: <https://ian.umces.edu/media-library/lutjanus-griseus-gray-snapper/> [Accessed 25 April 2023]
- Lamont, T.A.C., Williams, B., Chapuis, L., Prasetya, M.E., Seraphim, M.J., Harding, H.R. et al. (2022). The sound of recovery: Coral reef restoration success is detectable in the

- soundscape. *Journal of Applied Ecology*, **59**, 742–756. <https://doi.org/10.1111/1365-2664.14089>
- Ledoux, T., Clements, J.C., Comeau, L.A., Cervello, G., Tremblay, R., Olivier, F. et al. (2023). Effects of anthropogenic sounds on the behavior and physiology of the Eastern oyster (*Crassostrea virginica*). *Frontiers in Marine Science*, **10**, 1104526. <https://doi.org/10.3389/fmars.2023.1104526>
- Lee, K.M., Ballard, M.S., McNeese, A.R., Wilson, P.S., Venegas, G.R., Zeh, M.C. et al. (2023). Inter-seasonal comparison of acoustic propagation in a *Thalassia testudinum* seagrass meadow in a shallow sub-tropical lagoon. *JASA Express Letters*, **3**(1), 010801. <https://doi.org/10.1121/10.0016752>
- Lenth, R. (2022) emmeans: Estimated marginal means, aka least-squares means. R Package. Available at: <https://CRAN.R-project.org/package=emmeans> [Accessed 25 April 2023]
- Li, G., Wang, J., Liu, B., Meng, X., Kan, G. & Pei, Y. (2019). Measurement and modeling of high-frequency acoustic properties in fine sandy sediments. *Earth and Space Science*, **6**(11), 2057–2070. <https://doi.org/10.1029/2019ea000656>
- Lillis, A., Eggleston, D.B. & Bohnenstiehl, D.R. (2014a). Estuarine soundscapes: Distinct acoustic characteristics of oyster reefs compared to soft-bottom habitats. *Marine Ecology Progress Series*, **505**, 1–17. <https://doi.org/10.3354/meps10805>
- Lillis, A., Eggleston, D.B. & Bohnenstiehl, D.R. (2014b). Soundscape variation from a larval perspective: The case for habitat-associated sound as a settlement cue for weakly swimming estuarine larvae. *Marine Ecology Progress Series*, **509**, 57–70. <https://doi.org/10.3354/meps10917>



- Lillis, A., Perelman, J.N., Panyi, A. & Mooney, T.A. (2017). Sound production patterns of big-clawed snapping shrimp (*Alpheus* spp.) are influenced by time-of-day and social context. *The Journal of the Acoustical Society of America*, **142**(5), 3311–3320.  
<https://doi.org/10.1121/1.5012751>
- Lillis, A. & Mooney, T.A. (2018). Snapping shrimp sound production patterns on Caribbean coral reefs: Relationships with celestial cycles and environmental variables. *Coral Reefs*, **37**, 597–607. <https://doi.org/10.1007/s00338-018-1684-z>
- Lillis, A. & Mooney, T.A. (2022). Sounds of a changing sea: Temperature drives acoustic output by dominant biological sound-producers in shallow water habitats. *Frontiers in Marine Science*, **9**, 960881. <https://doi.org/10.3389/fmars.2022.960881>
- Lindseth, A.V. & Lobel, P.S. (2018). Underwater soundscape monitoring and fish bioacoustics: A review. *Fishes*, **3**(3), 36. <https://doi.org/10.3390/fishes3030036>
- Looby, A., Cox, K., Bravo, S., Rountree, R., Juanes, F., Reynolds, L.K. et al. (2022). A quantitative inventory of global soniferous fish diversity. *Reviews in Fish Biology and Fisheries*, **32**, 581–595. <https://doi.org/10.1007/s11160-022-09702-1>
- Looby, A., Vela, S., Cox, K., Riera, A., Bravo, S., Davies, H.L. et al. (2023). FishSounds Version 1.0: A website for the compilation of fish sound production information and recordings. *Ecological Informatics*, **74**, 101953.  
<https://doi.org/10.1016/j.ecoinf.2022.101953>
- Looby, A., Riera, A., Vela, S., Cox, K., Bravo, S., Rountree, R. et al. (2023). FishSounds, Version 2. Available at: <https://www.fishsounds.net> [Accessed 25 April 2023]
- Lyon, R.P., Eggleston, D.B., Bohnenstiehl, D.R., Layman, C.A., Ricci, S.W. & Allgeier, J.E. (2019). Fish community structure, habitat complexity, and soundscape characteristics of

- patch reefs in a tropical, back-reef system. *Marine Ecology Progress Series*, **609**, 33–48.  
<https://doi.org/10.3354/meps12829>
- Mackenzie, K.V. (1981). Nine-term equation for sound speed in the oceans. *The Journal of the Acoustical Society of America*, **70**(3), 807–812. <https://doi.org/10.1121/1.386920>
- Maricle, B.R. & Lee, R.W. (2002). Aerenchyma development and oxygen transport in the estuarine cordgrasses *Spartina alterniflora* and *S. anglica*. *Aquatic Botany*, **74**(2), 109–120. [https://doi.org/10.1016/s0304-3770\(02\)00051-7](https://doi.org/10.1016/s0304-3770(02)00051-7)
- Mathews, L.M. (2006). Cryptic biodiversity and phylogeographical patterns in a snapping shrimp species complex. *Molecular Ecology*, **15**(13), 4049–4063.  
<https://doi.org/10.1111/j.1365-294x.2006.03077.x>
- McAfee, D., Williams, B.R., McLeod, L., Reuter, A., Wheaton, Z. & Connell, S.D. (2023). Soundscape enrichment enhances recruitment and habitat building on new oyster reef restorations. *Journal of Applied Ecology*, **60**(3), 111–120. <https://doi.org/10.1111/1365-2664.14307>
- McIver, E.L., Marchaterre, M.A., Rice, A.N. & Bass, A.H. (2014). Novel underwater soundscape: Acoustic repertoire of plainfin midshipman fish. *Journal of Experimental Biology*, **217**(13), 2377–2389. <https://doi.org/10.1242/jeb.102772>
- Miksis-Olds, J.L. & Miller, J.H. (2006). Transmission loss in manatee habitats. *The Journal of the Acoustical Society of America*, **120**(4), 2320–2327. <https://doi.org/10.1121/1.2258832>
- Miksis-Olds, J.L., Dugan, P.J., Martin, S.B., Klinck, H., Mellinger, D.K., Mann, D.A. et al. (2021). Ocean sound analysis software for Making Ambient Noise Trends Accessible (MANTA). *Frontiers in Marine Science*, **8**, 703650.  
<https://doi.org/10.3389/fmars.2021.703650>

- Monczak, A., Mueller, C., Miller, M.E., Ji, Y., Borgianini, S.A. & Montie, E.W. (2019). Sound patterns of snapping shrimp, fish, and dolphins in an estuarine soundscape of the southeastern USA. *Marine Ecology Progress Series*, **609**, 49–68.  
<https://doi.org/10.3354/meps12813>
- Monczak, A., McKinney, B., Mueller, C. & Montie, E.W. (2020). What’s all that racket! Soundscapes, phenology, and biodiversity in estuaries. *PLoS ONE*, **15**(9), e0236874.  
<https://doi.org/10.1371/journal.pone.0236874>
- Moore, J.F., Pine, W.E., Frederick, P.C., Beck, S., Moreno, M., Dodrill, M.J. et al. (2020). Trends in oyster populations in the Northeastern Gulf of Mexico: An assessment of river discharge and fishing effects over time and space. *Marine and Coastal Fisheries*, **12**(3), 191–204. <https://doi.org/10.1002/mcf2.10117>
- Mullet, T.C., Farina, A. & Gage, S.H. (2017). The Acoustic Habitat Hypothesis: An ecoacoustics perspective on species habitat selection. *Biosemiotics*, **10**, 319–336.  
<https://doi.org/10.1007/s12304-017-9288-5>
- National Oceanic and Atmospheric Administration. (2015). *Guidance for Considering the Use of Living Shorelines*. Available at: [https://www.habitatblueprint.noaa.gov/wp-content/uploads/2018/01/NOAA-Guidance-for-Considering-the-Use-of-Living-Shorelines\\_2015.pdf](https://www.habitatblueprint.noaa.gov/wp-content/uploads/2018/01/NOAA-Guidance-for-Considering-the-Use-of-Living-Shorelines_2015.pdf) [Accessed 25 April 2023]
- Nedelec, S.L., Campbell, J., Radford, A.N., Simpson, S.D. & Merchant, N.D. (2016). Particle motion: The missing link in underwater acoustic ecology. *Methods in Ecology and Evolution*, **7**(7), 836–842. <https://doi.org/10.1111/2041-210x.12544>
- Nyborg, W.L. & Rudnick, I. (1948). Acoustic absorption in sand and soil. *The Journal of the Acoustical Society of America*, **20**(4), 597–598. <https://doi.org/10.1121/1.1917021>

- O'Donnell, J.E.D. (2017). Living shorelines: A review of literature relevant to New England coasts. *Journal of Coastal Research*, **33**(2), 435–451. <https://doi.org/10.2112/jcoastres-d-15-00184.1>
- Olsen Associates, Inc. (2007). *Feasibility Study of Beach Improvements: 1st and G Streets, Cedar Key, FL*
- Okasanen, J., Simpson, G.L., Blanchet, F.G., Kindt, R., Legendre, P., Minchin, P.R. et al. (2022). vegan: Community Ecology Package. R Package. Available at: <https://cran.r-project.org/web/packages/vegan/vegan.pdf> [Accessed 25 April 2023]
- Pijanowski, B.C., Farina, A., Gage, S.H., Dumyahn, S.L. & Krause, B.L. (2011). What is soundscape ecology? An introduction and overview of an emerging new science. *Landscape Ecology*, **26**, 1213–1232. <https://doi.org/10.1007/s10980-011-9600-8>
- Polk, M.A., Gittman, R.K., Smith, C.S. & Eulie, D.O. (2022). Coastal resilience surges as living shorelines reduce lateral erosion of salt marshes. *Integrated Environmental Assessment and Management*, **18**(1), 82–98. <https://doi.org/10.1002/ieam.4447>
- Popper, A.N. & Hawkins, A.D. (2018). The importance of particle motion to fishes and invertebrates. *The Journal of the Acoustical Society of America*, **143**(1), 470–488. <https://doi.org/10.1121/1.5021594>
- Popper, A.N., Hawkins, A.D. & Sisneros, J.A. (2022). Fish hearing “specialization” – A re-evaluation. *Hearing Research*, **425**, 108393. <https://doi.org/10.1016/j.heares.2021.108393>
- Ricci, S.W., Eggleston, D.B., Bohnenstiehl, D.R. & Lillis, A. (2016). Temporal soundscape patterns and processes in an estuarine reserve. *Marine Ecology Progress Series*, **550**, 25–38. <https://doi.org/10.3354/meps11724>

- Ridge, J.T., Rodriguez, A.B., Fodrie, F.J., Lindquist, N.L., Brodeur, M.C., Coleman, S.E. et al. (2015). Maximizing oyster-reef growth supports green infrastructure with accelerating sea-level rise. *Scientific Reports*, **5**, 14785. <https://doi.org/10.1038/srep14785>
- Rogers, P.H. & Cox, M. (1988). Underwater sound as a biological stimulus. In: Atema, J., Fay, R.R., Popper, A.N. & Tavolga, W.N. (eds) *Sensory Biology of Aquatic Animals*. Springer, New York
- R Core Team. (2022). R: A language and environment for statistical computing. *R Foundation for Statistical Computing*, Vienna, Austria. Available at: <https://www.R-project.org/> [Accessed 25 April 2023]
- Salas, A.K., Wilson, P.S. & Fuiman, L.A. (2019). Ontogenetic change in predicted acoustic pressure sensitivity in larval red drum (*Sciaenops ocellatus*). *Journal of Experimental Biology*, **222**(16), jeb201962. <https://doi.org/10.1242/jeb.201962>
- Saxby, T. (2004). *Spartina* spp. (salt marsh grass). *IAN/UMCES Symbol and Image Libraries*. Available at: <https://ian.umces.edu/media-library/spartina-spp-salt-marsh-grass/> [Accessed 25 April 2023]
- Saxby, T. (2006a). Oyster 3D reef. *IAN/UMCES Symbol and Image Libraries*. Available at: <https://ian.umces.edu/media-library/oyster-3d-reef/> [Accessed 25 April 2023]
- Saxby, T. (2006b). Oyster shell bag. *IAN/UMCES Symbol and Image Libraries*. Available at: <https://ian.umces.edu/media-library/oyster-shell-bag/> [Accessed 25 April 2023]
- Saxby, T. (2008). *Bairdiella chrysoura* (American silver perch). *IAN/UMCES Symbol and Image Libraries*. Available at: <https://ian.umces.edu/media-library/bairdiella-chrysoura-american-silver-perch/> [Accessed 25 April 2023]

- Short, F.T., Kosten, S., Morgan, P.A., Malone, S. & Moore, G.E. (2016). Impacts of climate change on submerged and emergent wetland plants. *Aquatic Botany*, **135**, 3–17.  
<https://doi.org/10.1016/j.aquabot.2016.06.006>
- Smith, C.S., Puckett, B., Gittman, R.K. & Peterson, C.H. (2018). Living shorelines enhanced the resilience of saltmarshes to Hurricane Matthew (2016). *Ecological Applications*, **28**(4), 871–877. <https://doi.org/10.1002/eap.1722>
- Smith, C.S., Rudd, M.E., Gittman, R.K., Melvin, E.C., Patterson, V.S., Renzi, J.J. et al. (2020). Coming to terms with living shorelines: A scoping review of novel restoration strategies for shoreline protection. *Frontiers in Marine Science*, **7**, 434.  
<https://doi.org/10.3389/fmars.2020.00434>
- Smith, C.S., Paxton, A.B., Donaher, S.E., Kochan, D.P., Neylan, I.P., Pfeifer, T. et al. (2021). Acoustic camera and net surveys reveal that nursery enhancement at living shorelines may be restricted to the marsh platform. *Ecological Engineering*, **166**, 106232.  
<https://doi.org/10.1016/j.ecoleng.2021.106232>
- Solé, M., Kaifu, K., Mooney, T.A., Nedelec, S.L., Olivier, F., Radford, A.N. et al. (2023a). Marine invertebrates and noise. *Frontiers in Marine Science*, **10**, 1129057.  
<https://doi.org/10.3389/fmars.2023.1129057>
- Solé, M., Vreese, S.D., Sánchez, A.M., Fortuño, J.-M., Schaar, M. van der, Sancho, N. et al. (2023b). Cross-sensory interference assessment after exposure to noise shows different effects in the blue crab olfactory and sound sensing capabilities. *Science of The Total Environment*, **873**, 162260. <https://doi.org/10.1016/j.scitotenv.2023.162260>
- Song, Z., Salas, A.K., Montie, E.W., Laferriere, A., Zhang, Y. & Mooney, T.A. (2021). Sound pressure and particle motion components of the snaps produced by two snapping shrimp

- species (*Alpheus heterochaelis* and *Alpheus angulosus*). *The Journal of the Acoustical Society of America*, **150**(5), 3288–3301. <https://doi.org/10.1121/10.0006973>
- Stewart-Oaten, A., Bence, J.R. & Osenberg, C.W. (1992). Assessing effects of unreplicated perturbations: No simple solutions. *Ecology*, **73**(4), 1396–1404. <https://doi.org/10.2307/1940685>
- The MathWorks Inc. (2022). MATLAB version: 9.13.0 (R2022b), Natick, Massachusetts: The MathWorks Inc. Available at: <https://www.mathworks.com> [Accessed 15 October 2022]
- Thomas, J. (2003). *Callinectes sapidus* (blue crab): Adult 2. *IAN/UMCES Symbol and Image Libraries*. Available at: <https://ian.umces.edu/media-library/callinectes-sapidus-blue-crab-adult-2/> [Accessed 25 April 2023]
- Thomas, J. (2004). *Limulus polyphemus* (horseshoe crab). *IAN/UMCES Symbol and Image Libraries*. Available at: <https://ian.umces.edu/media-library/limulus-polyphemus-horseshoe-crab/> [Accessed 25 April 2023]
- Toft, J.D., Dethier, M.N., Howe, E.R., Buckner, E.V. & Cordell, J.R. (2021). Effectiveness of living shorelines in the Salish Sea. *Ecological Engineering*, **167**, 106255. <https://doi.org/10.1016/j.ecoleng.2021.106255>
- Tracey, D. (2003). Prawn shrimp. *Water and Rivers Commission and IAN/UMCES Symbol and Image Libraries*. <https://ian.umces.edu/media-library/prawn-shrimp/> [Accessed 25 April 2023]
- Underwood, A.J. (1992). Beyond BACI: The detection of environmental impacts on populations in the real, but variable, world. *Journal of Experimental Marine Biology and Ecology*, **161**(2), 145–178. [https://doi.org/10.1016/0022-0981\(92\)90094-q](https://doi.org/10.1016/0022-0981(92)90094-q)

- Valiela, I., Bowen, J.L. & York, J.K. (2001). Mangrove forests: One of the world's threatened major tropical environments: At least 35% of the area of mangrove forests has been lost in the past two decades, losses that exceed those for tropical rain forests and coral reefs, two other well-known threatened environments. *BioScience*, **51**(10), 807–815.  
[https://doi.org/10.1641/0006-3568\(2001\)051\[0807:mfootw\]2.0.co;2](https://doi.org/10.1641/0006-3568(2001)051[0807:mfootw]2.0.co;2)
- van Geel, N.C.F., Risch, D. & Wittich, A. (2022). A brief overview of current approaches for underwater sound analysis and reporting. *Marine Pollution Bulletin*, **178**, 113610.  
<https://doi.org/10.1016/j.marpolbul.2022.113610>
- Vieira, M., Fonseca, P.J., & Amorim, M.C.P. (2021). Fish sounds and boat noise are prominent soundscape contributors in an urban European estuary. *Marine Pollution Bulletin*, **172**, 112845. <https://doi.org/10.1016/j.marpolbul.2021.112845>
- Wall, C.C., Haver, S.M., Hatch, L.T., Miksis-Olds, J., Bochenek, R., Dziak, R.P. & Gedamke, J. (2021). The next wave of passive acoustic data management: How centralized access can enhance science. *Frontiers in Marine Science*, **8**, 703682.  
<https://doi.org/10.3389/fmars.2021.703682>
- Wang, J., Li, G., Kan, G., Hou, Z., Meng, X., Liu, B. et al. (2021). High frequency dependence of sound speed and attenuation in coral sand sediments. *Ocean Engineering*, **234**, 109215. <https://doi.org/10.1016/j.oceaneng.2021.109215>
- Waycott, M., Duarte, C.M., Carruthers, T.J.B., Orth, R.J., Dennison, W.C., Olyarnik, S. et al. (2009). Accelerating loss of seagrasses across the globe threatens coastal ecosystems. *Proceedings of the National Academy of Sciences*, **106**(30), 12377–12381.  
<https://doi.org/10.1073/pnas.0905620106>



- Wickham H, Chang, W., Henry, L., Pedersen, T.L., Takahashi, K., Wilke, C. et al. (2023) *ggplot2*: Create elegant data visualisations using the grammar of graphics. R Package. Available at: <https://cran.r-project.org/web/packages/emmeans/emmeans.pdf> [Accessed 25 April 2023]
- Williams, B.R., McAfee, D. & Connell, S.D. (2021). Repairing recruitment processes with sound technology to accelerate habitat restoration. *Ecological Applications*, **31**(6), e2386. <https://doi.org/10.1002/eap.2386>
- Williams, B.R., McAfee, D. & Connell, S.D. (2022). Oyster larvae swim along gradients of sound. *Journal of Applied Ecology*, **59**(7), 1815–1824. <https://doi.org/10.1111/1365-2664.14188>
- Wilson, L., Pine, M.K. & Radford, C.A. (2022). Small recreational boats: A ubiquitous source of sound pollution in shallow coastal habitats. *Marine Pollution Bulletin*, **174**, 113295. <https://doi.org/10.1016/j.marpolbul.2021.113295>
- Yang, J. & Tang, D. (2016). Direct measurements of sediment sound speed and attenuation in the frequency band of 28 kHz at the target and reverberation experiment site. *IEEE Journal of Oceanic Engineering*, **42**(4), 1102–1109. <https://doi.org/10.1109/joe.2017.2714722>

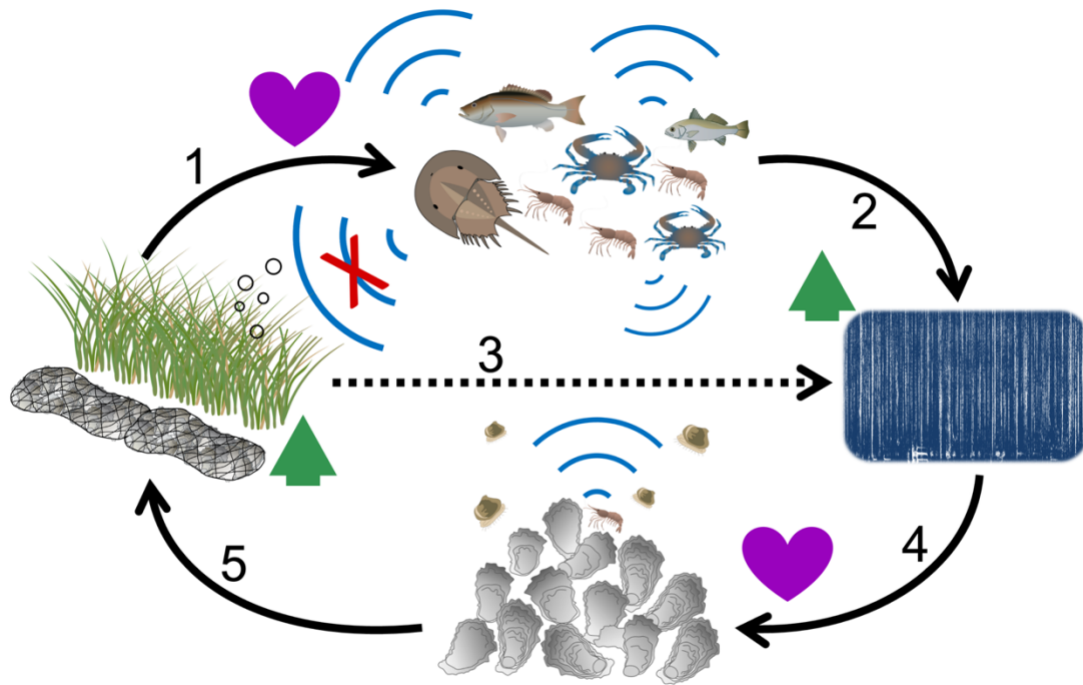


**FIGURE 1** A conceptual diagram showing hypothesized acoustically mediated benefits after a living shoreline construction. Following habitat enhancement, living shorelines are expected to have increased nekton populations, including some sound-producers (1), which would lead to an overall louder soundscape (2) provided acoustic propagation is not excessively reduced by the habitat structures (3). These soundscape changes would attract greater settlement (4) leading to further shoreline development (5). Images used with permission (Thomas, 2003, 2004; Tracey, 2003; Saxby, 2004, 2006a, 2006b, 2008; Kraeer & Essen-Fishman, 2008; Donovan, 2014; Integration and Application Network, 2023).

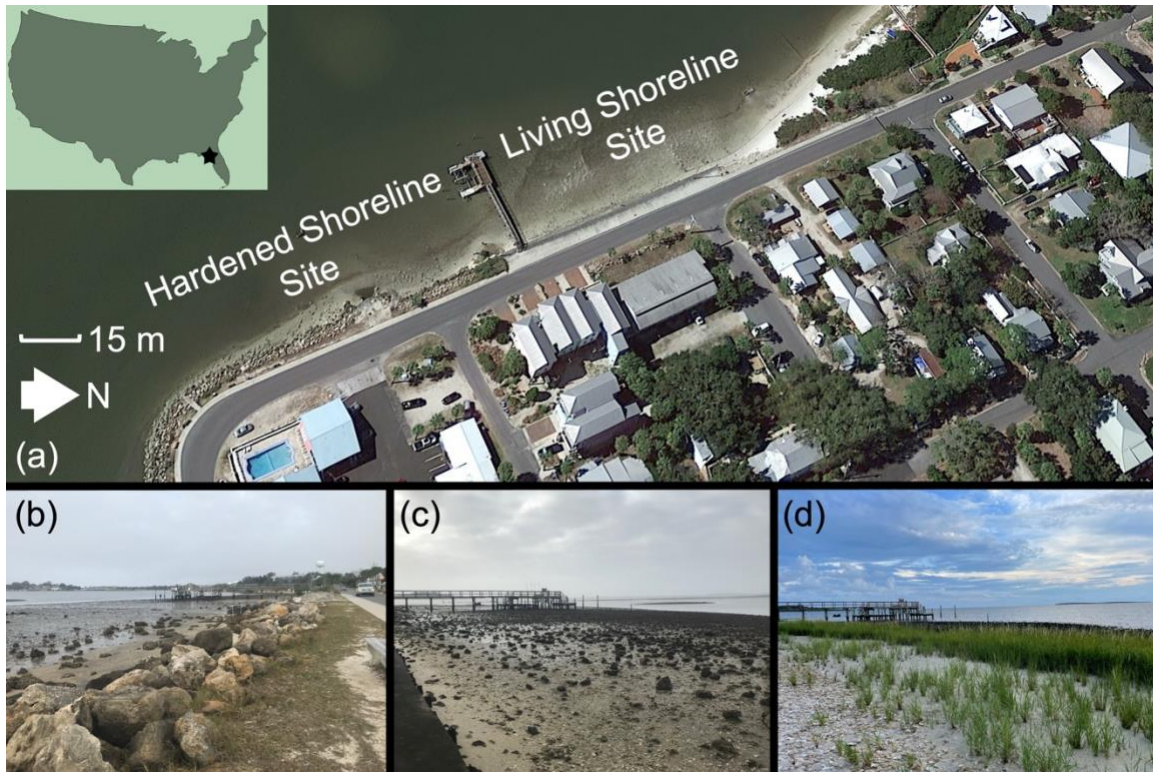


**FIGURE 2** Map and photos of the hardened and living shoreline sites studied. (a) Map showing the position of G Street Living Shoreline Restoration, created as part of the Daughtry Bayou Shoreline Project in Cedar Key, FL (USA), and the nearby hardened shoreline used as a reference site. Photos taken of the (b) hardened shoreline site and the (c) living shoreline site at low tide on 13 January 2020—prior to the living shoreline construction. (d) Photo taken of the living shoreline site at low tide on 16 September 2021—13 months after the initial living shoreline construction. Image used with permission (Google Earth Pro, 2023).

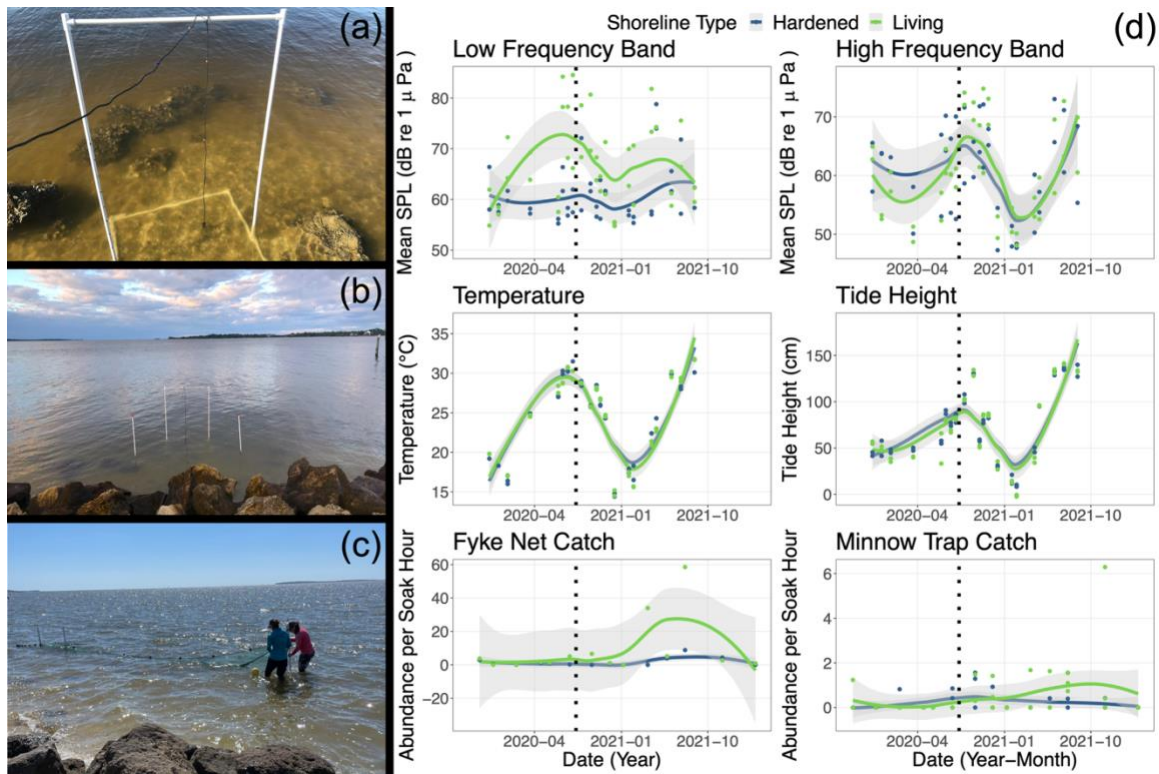


**FIGURE 3** Overview of the methods and results of the Before-After-Control-Impact (BACI) acoustic and nekton sampling. Photos showing the BACI acoustic sampling (a) deployment and (b) observer vantage position. (c) Photo showing the BACI nekton sampling fyke net deployment. All three photos were taken at the hardened shoreline site but at different sampling locations. (d) Results of the BACI sampling showing the mean received sound pressure level (SPL) of the low and high frequency bands (top), the recorded temperatures and measured tide heights associated with the BACI acoustic sampling (middle), and the abundance per soak time hour of the fyke net catches and minnow trap catches (bottom). The data were divided by site type, with the hardened shoreline represented by dark blue and the living shoreline represented by light green. Data lines were plotted with local polynomial regression fitting. The 95% confidence intervals are shown in gray. The vertical dotted lines denote the date of the initial living shoreline construction.



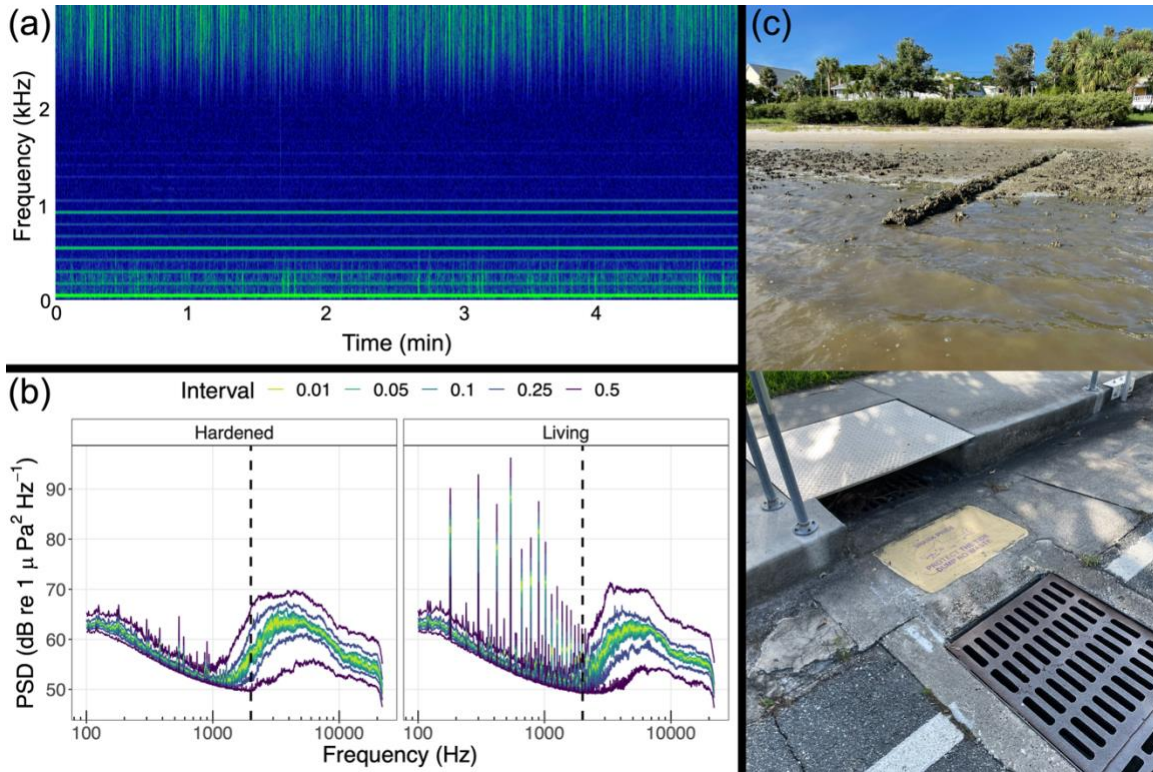


**FIGURE 4** (a) A representative spectrogram showing the relative amplitude (in brighter green) and frequency over time of the anthropogenic sound occasionally detected at the living shoreline site during the Before-After-Control-Impact (BACI) acoustic sampling. The anthropogenic sound was generally only detectable below 2 kHz, while the lower portion of the high frequency band is also shown for reference. The spectrogram was created in Raven Pro 1.6 with Default 1.3 Power settings, with brightness set to 35, contrast set to 64, and spectrogram window size set to 520 (K. Lisa Yang Center for Conservation Bioacoustics at the Cornell Lab of Ornithology, 2023). (b) Power spectral density (PSD) plots of all the BACI acoustic sampling recordings combined, with panels separating recordings taken at the hardened shoreline site (left) and living shoreline site (right). The vertical dashed lines delineate the low and high frequency bands used in the statistical analysis. (c) Photos of the location of the suspected source of the anthropogenic sound—a stormwater drainage pipe situated near the living shoreline site. Photo of the pipe (top) was taken at low tide (the pipe was usually fully submerged during BACI acoustic sampling).

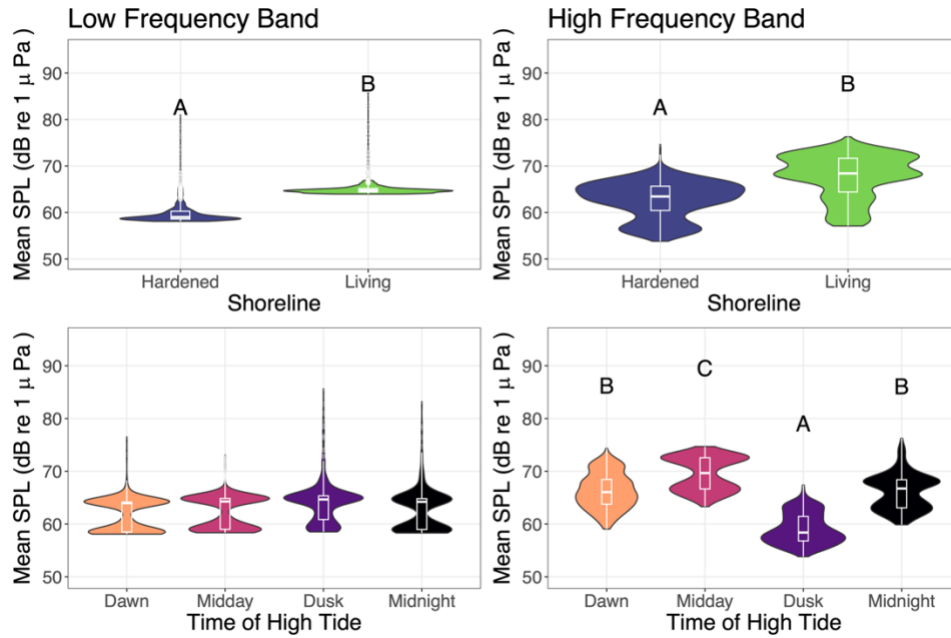


**FIGURE 5** Violin and box plots showing the results of the diel acoustic sampling about a year following initial living shoreline construction. The panels separate the data between the low (left) and high (right) frequency bands and the data divided by site type (top) and temporal window based on the time of high tide (bottom). The capital letters represent statistically significant differences ( $p \leq 0.05$ ).

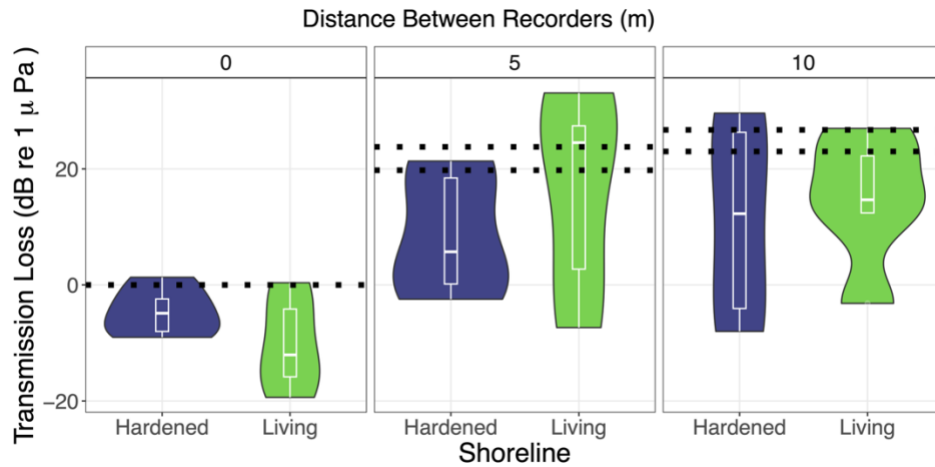


**FIGURE 6** Violin and box plots showing the results of the acoustic attenuation sampling when the difference between the recorders' distances from the speaker was 0 m, 5 m, and 10 m. Expected transmission loss ranges for each distance are shown with the dotted lines, based on a cylindrical spreading model accounting for the distance between recorders and the mean water depth at their locations.

**Intertidal Soundscapes of Hardened and Living Shorelines: A Case Study of Habitat  
Enhancement**

Audrey Looby\*, Laura K. Reynolds, Ashley M. McDonald, Savanna Barry, Mark Clark, Charles  
W. Martin

Journal title: Aquatic Conservation: Marine and Freshwater Ecosystems

\*Corresponding author: Audrey Looby, [alooby101@gmail.com](mailto:alooby101@gmail.com)

Fisheries and Aquatic Sciences, University of Florida, Gainesville, FL, USA

UF/IFAS Nature Coast Biological Station, University of Florida, Cedar Key, FL, USA

ORCID: <https://orcid.org/0000-0003-1833-8643>

Supporting Information: Figures S1–S12 and Tables S1 and S2





**FIGURE S1** Aerial photos of the living shoreline site taken on (a) 21 October 2017 (prior to construction), (b) 20 November 2020 (~3 months following initial construction), (c) 12 May 2021 (~9 months following initial construction and 1 week prior to secondary additions), and (d) 26 September 2022 (~2 years following initial construction and ~16 months following secondary additions).

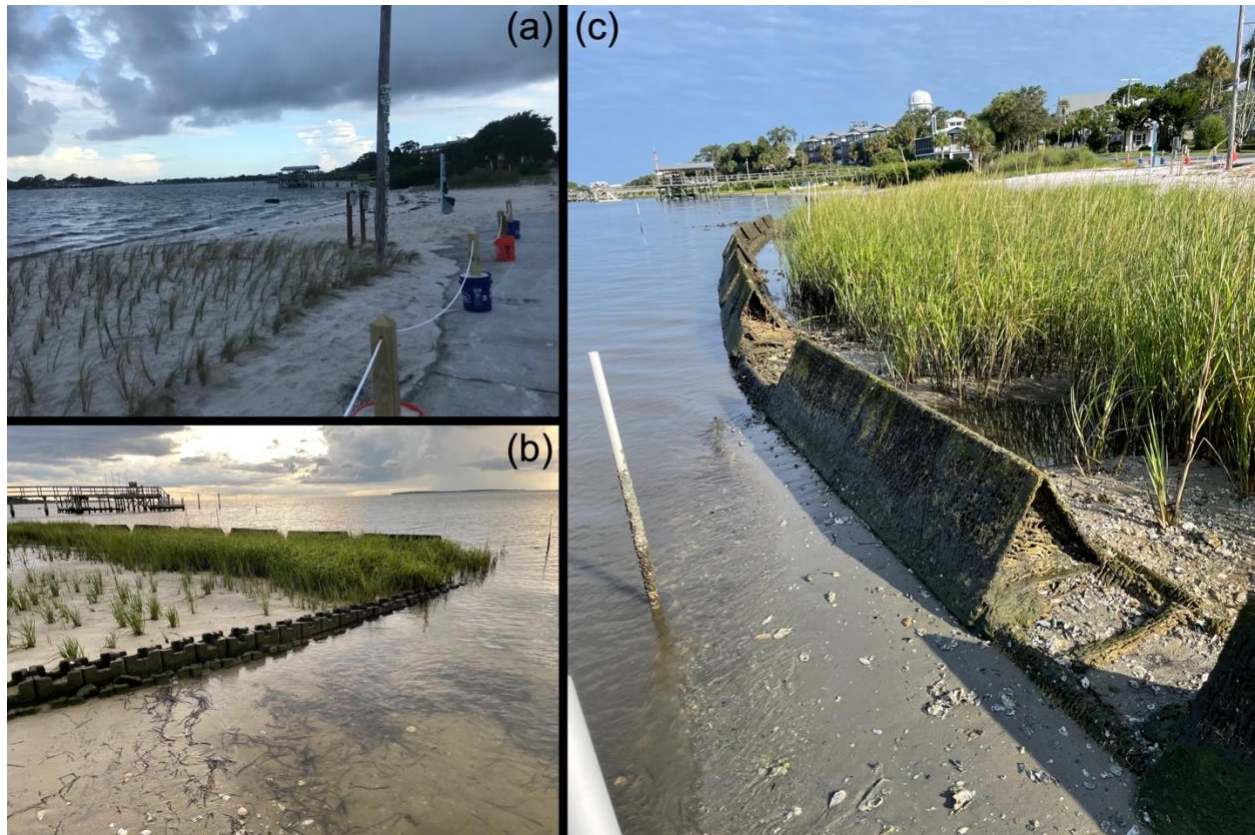


**FIGURE S2** Photos of the living shoreline site highlighting the (a) recreational beach area next to the salt marsh planting (taken on 31 August 2020), (b) the castle block installations (taken on 12 August 2021), and (c) the reef prism installations (taken on 13 September 2021).

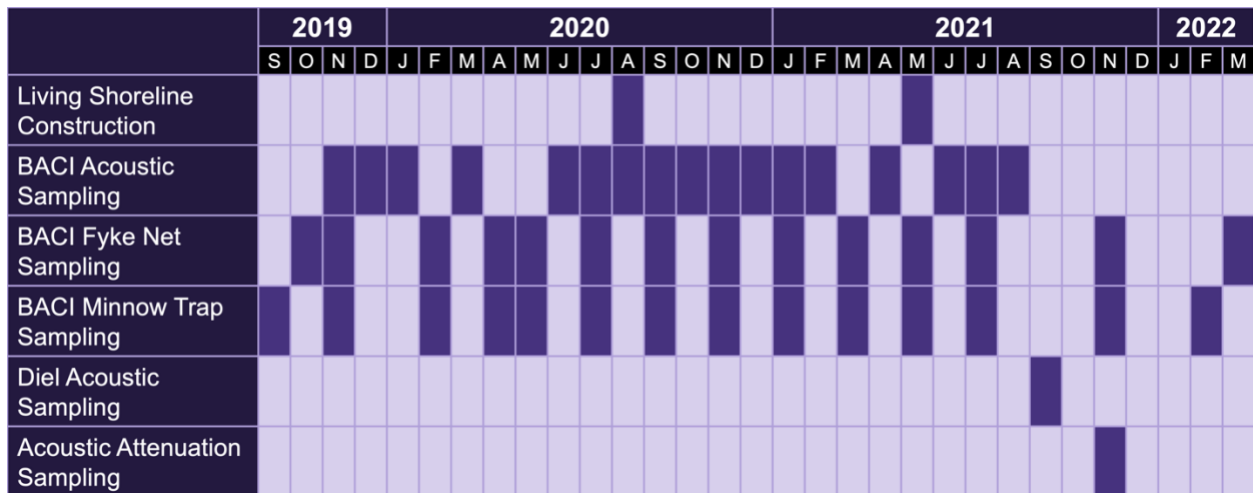


**FIGURE S3** Gantt chart showing the months and years in which the initial and additional living shoreline constructions as well as the various sampling methodologies occurred with darker colored boxes. Multiple Before-After-Control-Impact (BACI) acoustic sampling events may have occurred in the same month.





**FIGURE S4** Map of the approximate acoustic sampling locations at the hardened and living shoreline sites. Before-After-Control-Impact (BACI) snapshot acoustic sampling occurred at locations 1, 2, 3, and 4. Diel acoustic sampling occurred at locations 5 and 6. Acoustic attenuation sampling occurred along transects, approximately represented with light blue lines. The location of the suspected source of the anthropogenic sound—an abandoned stormwater drainage pipe—is situated to the north of the living shoreline site. Image used with permission (Google Earth Pro, 2023).

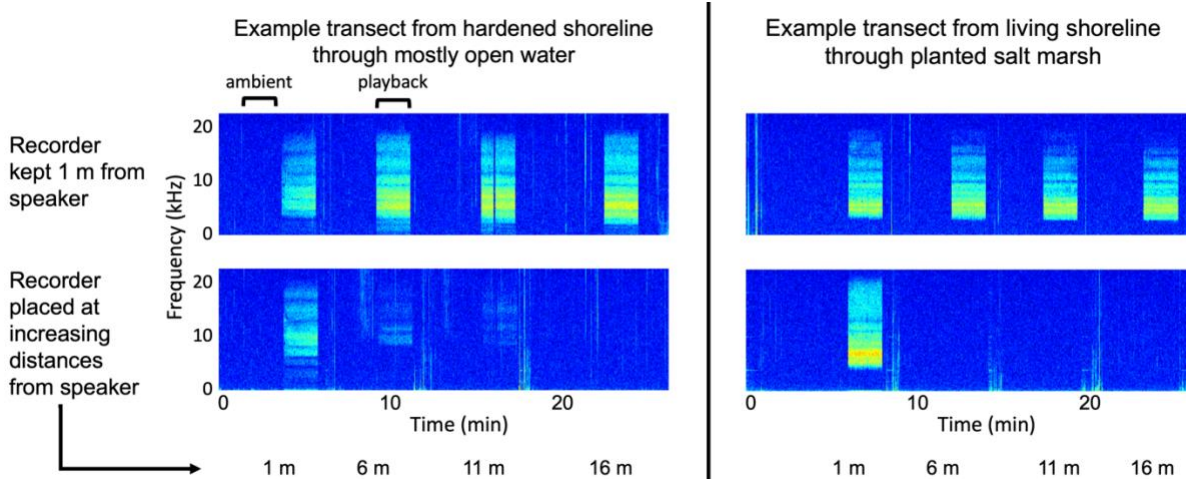


**FIGURE S5** Spectrograms of example recordings collected during the acoustic attenuation field sampling. Both example transects were ones that ran roughly parallel to shore. The spectrograms were created in Raven Pro 1.6 with Default 1.3 Power settings with brightness, contrast, and spectrogram window size kept consistent among them (K. Lisa Yang Center for Conservation Bioacoustics at the Cornell Lab of Ornithology, 2023). The spectrogram visualizations do not incorporate sensitivity differences between the two recorders used and do not illustrate the variation found among other transects conducted within the two sites, and so they should therefore be interpreted cautiously.

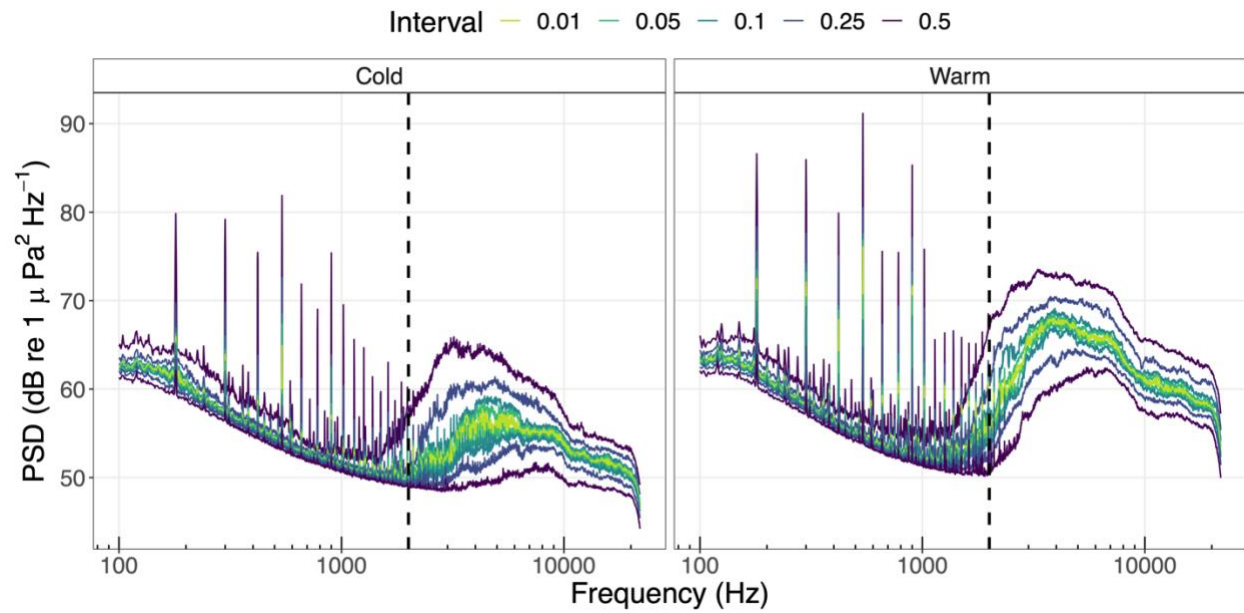


**FIGURE S6** Power spectral density (PSD) plots of all the Before-After-Control-Impact acoustic sampling recordings combined, with panels separating recordings taken during the cold season (left) and warm season (right). The vertical dashed lines delineate the low and high frequency bands used in the statistical analysis.

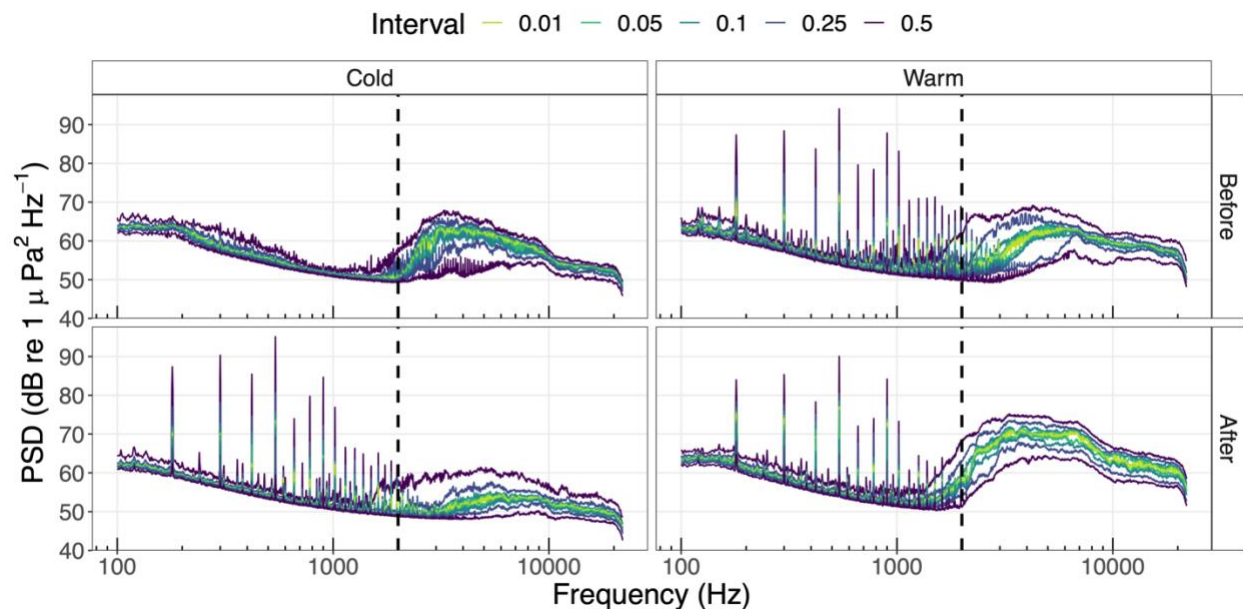


**FIGURE S7** Power spectral density (PSD) plots of all the Before-After-Control-Impact acoustic sampling recordings combined, with panels separating recordings taken before (top) and after (bottom) the initial living shoreline construction and during the cold season (left) and warm season (right). The vertical dashed lines delineate the low and high frequency bands used in the statistical analysis.

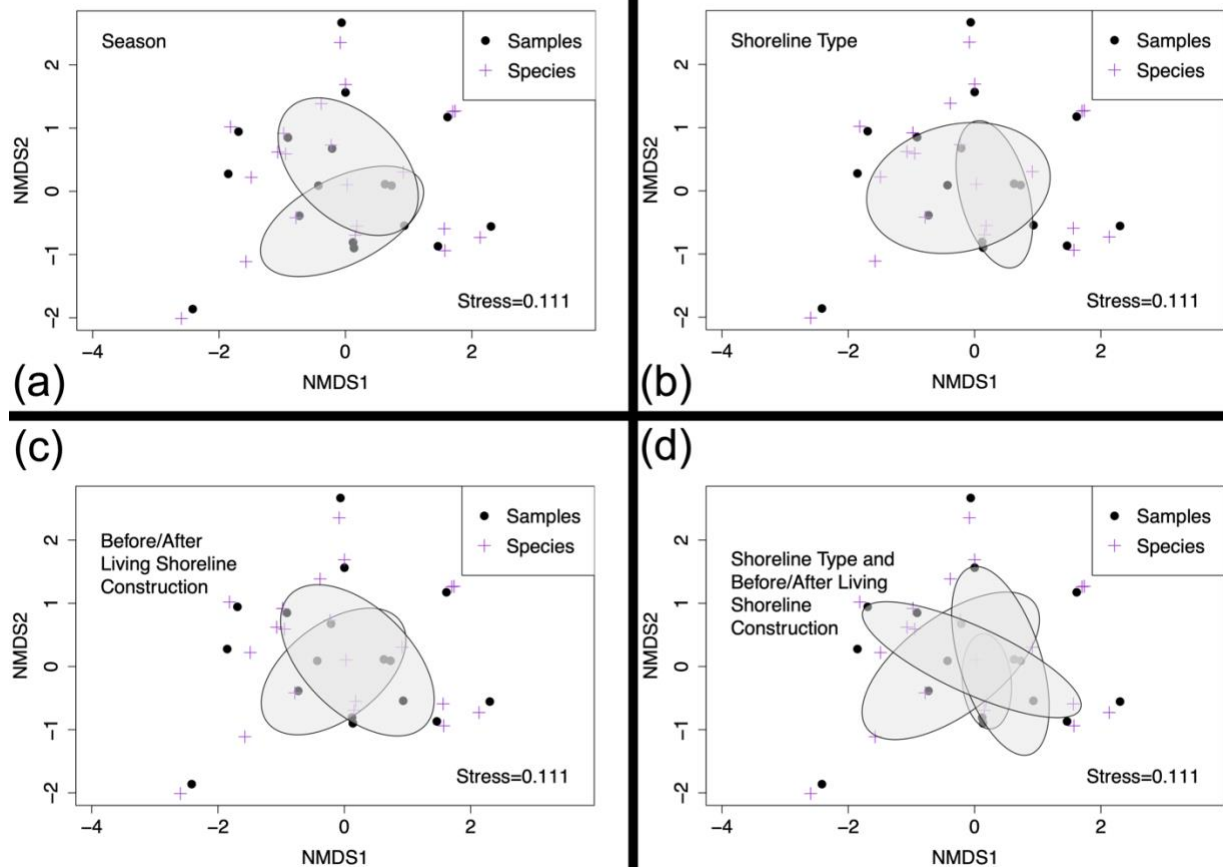


**FIGURE S8** Nonmetric multidimensional scaling (NMDS) plots of the nekton sampling fyke net community data plotted as abundance per soak time hour in two dimensions with ellipses representing (a) warm and cold seasons, (b) the two shoreline types, (c) before and after the living shoreline construction, and (d) both the shoreline types and before and after the living shoreline construction.



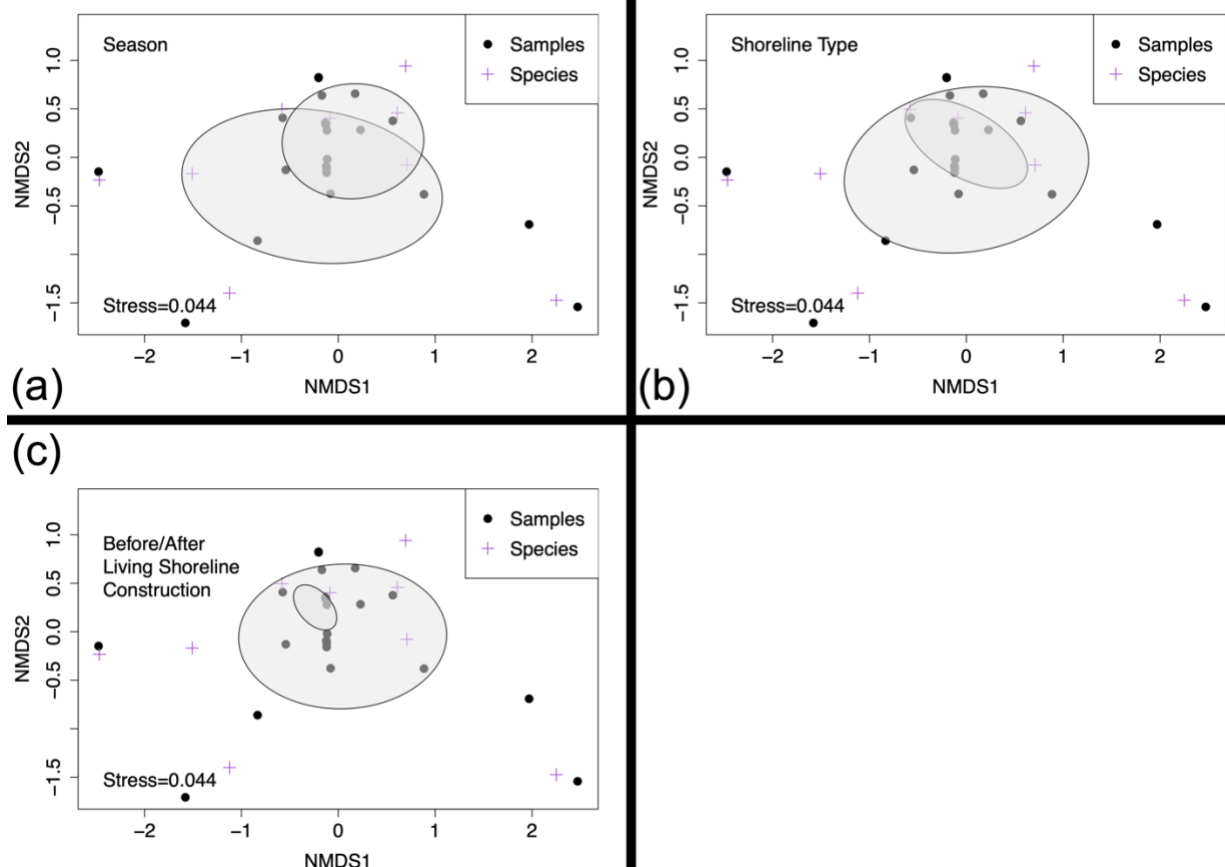


**FIGURE S9** Nonmetric multidimensional scaling (NMDS) plots of the nekton sampling minnow trap community data plotted as abundance per soak time hour in two dimensions with ellipses representing (a) warm and cold seasons, (b) the two shoreline types, and (c) before and after the living shoreline construction. Ellipses representing both the shoreline types and before and after the living shoreline construction could not be visualized because of too few samples with non-zero catch in some of the categories.

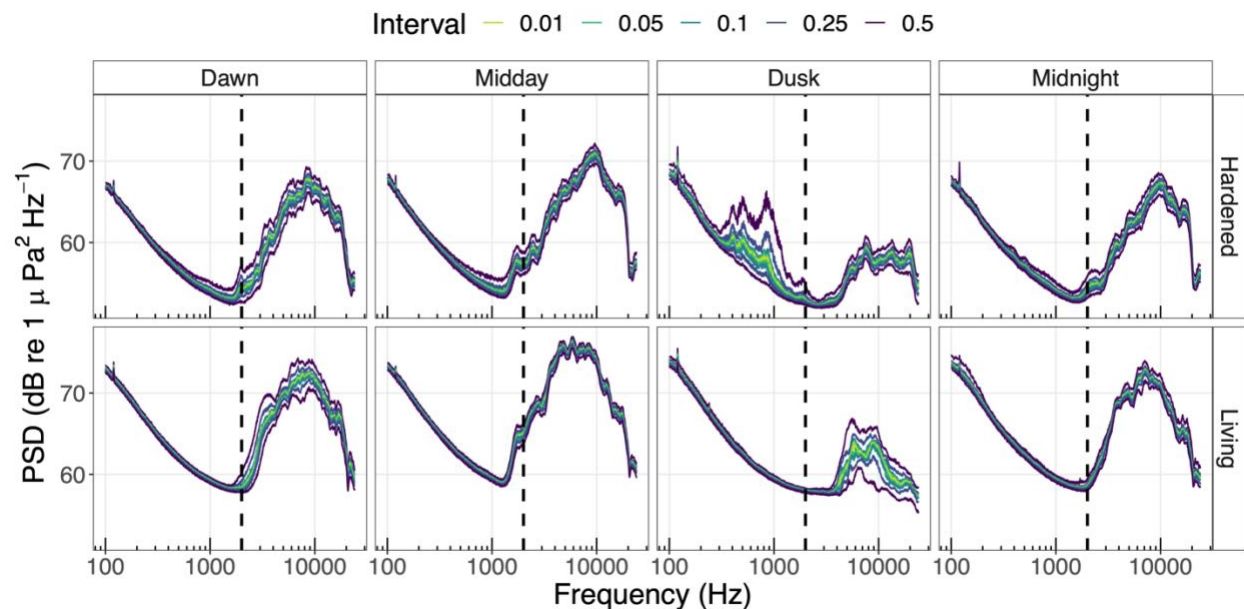


**FIGURE S10** Power spectral density (PSD) plots of all the diel acoustic sampling recordings, with panels separating recordings taken at the hardened shoreline site (top) and living shoreline site (bottom) as well as the temporal windows (dawn, midday, dusk, and midnight from left to right). The vertical dashed lines delineate the low and high frequency bands used in the statistical analysis.

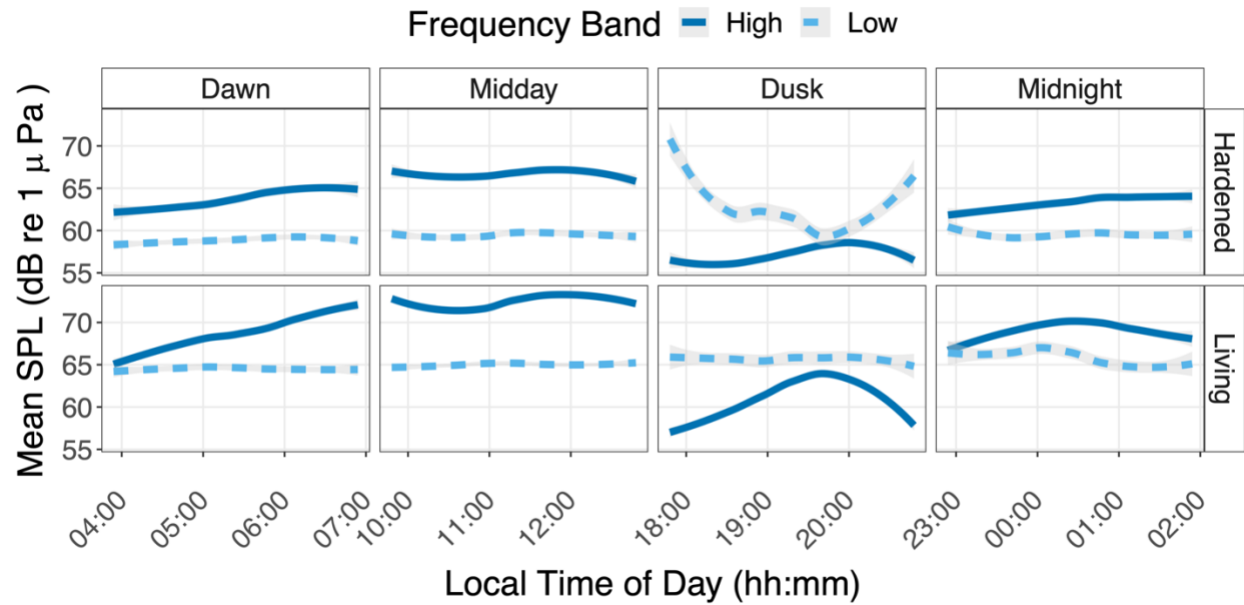


**FIGURE S11** The mean received sound pressure level (SPL) of the low (light blue, dashed line) and high frequency (dark blue, solid line) bands recorded during the diel acoustic sampling. The panels separate recordings taken at the hardened shoreline site (top) and living shoreline site (bottom) as well as the temporal windows (dawn, midday, dusk, and midnight from left to right). Data lines were plotted with local polynomial regression fitting. The 95% confidence intervals are shown in gray.

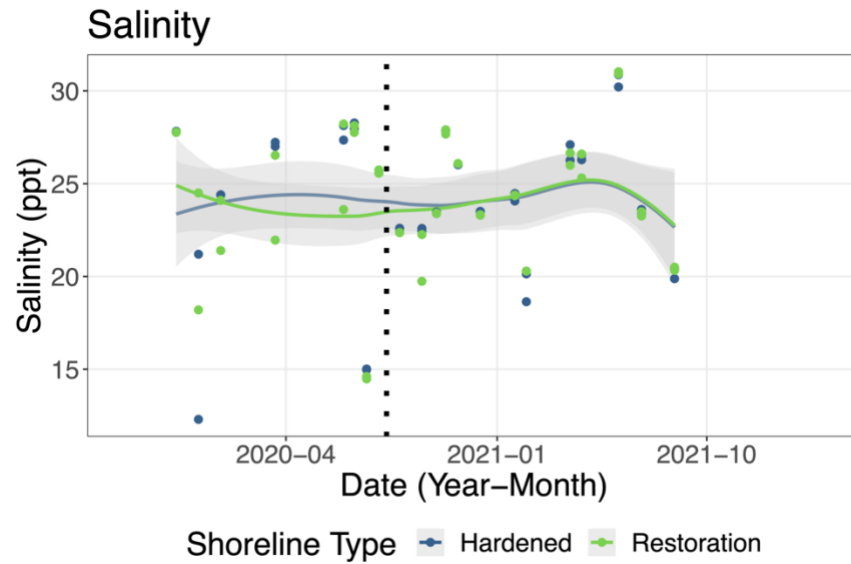


**FIGURE S12** The recorded salinity associated with the Before-After-Control-Impact acoustic sampling. The data were divided by site type, with the hardened shoreline represented by dark blue and the living shoreline represented by light green. Data lines were plotted with local polynomial regression fitting. The 95% confidence intervals are shown in gray. The vertical dotted line denotes the date of the initial living shoreline construction.

**TABLE S1** The results of the Before-After-Control-Impact acoustic sampling high frequency band mixed effects model comparison. npar denotes the number of parameters, AIC denotes the Akaike information criterion, BIC denotes the Bayesian information criterion, LogLik denotes the log-likelihood, and df denotes the degrees of freedom.

<b>Model</b>	<b>npar</b>	<b>AIC</b>	<b>BIC</b>	<b>LogLik</b>	<b>Deviance</b>	<b>X<sup>2</sup></b>	<b>df</b>	<b>Pr (&gt;X<sup>2</sup>)</b>
Null	3	-108.14	-100.84	57.068	-114.14			
Full	10	-142.66	-118.36	81.332	-162.66	48.528	7	< 0.001

**TABLE S2** The results of the Before-After-Control-Impact acoustic sampling low frequency band mixed effects model comparison. npar denotes the number of parameters, AIC denotes the Akaike information criterion, BIC denotes the Bayesian information criterion, LogLik denotes the log-likelihood, and df denotes the degrees of freedom.

<b>Model</b>	<b>np</b>	<b>par</b>	<b>AIC</b>	<b>BIC</b>	<b>LogLik</b>	<b>Deviance</b>	<b>X<sup>2</sup></b>	<b>df</b>	<b>Pr (&gt;X<sup>2</sup>)</b>
Null	3		-137.29	-130.00	71.646	-143.29			
Full	10		-135.54	-111.23	77.771	-155.54	12.249	7	0.09265

## References

- Google Earth Pro. (2023). Cedar Key, FL. 29° 08' 06.2"N, 83° 02' 10.8"W, Eye Alt 271 m, Imagery Date February 7, 2020. *TerraMetrics 2023, Google Earth Pro V 7.3.6* [Accessed March 28, 2023]
- K. Lisa Yang Center for Conservation Bioacoustics at the Cornell Lab of Ornithology. (2023). Raven Pro: Interactive sound analysis software. Available at: <https://ravensoundsoftware.com/> [Accessed 25 April 2023]